

# **Numerical simulation of the application of Fe<sub>3</sub>O<sub>4</sub> nanofluid in photovoltaic thermal collector system**

Submitted By

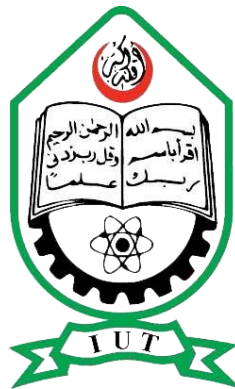
**Naimul Islam**

180011206

Supervised By

**Dr. Md. Rezwatul Karim**

**A Thesis submitted in partial fulfillment of the requirement for the degree of Bachelor of Science in Mechanical Engineering**



Department of Mechanical and Production Engineering (MPE)

Islamic University of Technology (IUT)

May, 2023

## **Candidate's Declaration**

This is to certify that the work presented in this thesis, titled, “Numerical simulation of the application of Fe<sub>3</sub>O<sub>4</sub> nanofluid in photovoltaic thermal collector system”, is the outcome of the investigation and research carried out by me under the supervision of Dr. Md. Rezwanul Karim, Associate Professor, MPE Dept., IUT, Board Bazar, Gazipur-1704, Bangladesh.

It is also declared that neither this thesis nor any part of it has been submitted elsewhere for the award of any degree or diploma.

Naimul Islam

-----

Name of the Student

Student No: 180011206

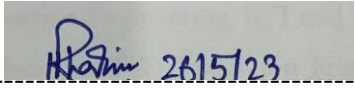
## Recommendation of the board of supervisors

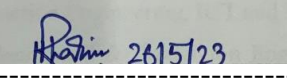
---

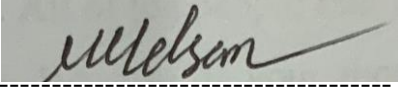
The thesis titled “Numerical simulation of the application of Fe<sub>3</sub>O<sub>4</sub> nanofluid in photovoltaic thermal collector system” submitted by Naimul Islam, Student No: 180011206, has been accepted as satisfactory in partial fulfillment of the requirements for the degree of BSc. in Mechanical Engineering on 19<sup>th</sup> MAY, 2023.

## Board of Examiners

---

1.  (Thesis Supervisor)  
Dr. Md. Rezwanul Karim  
Associate Professor  
MPE Dept., IUT, Board Bazar, Gazipur-1704, Bangladesh.

2. For  (Examiner – 1)  
Dr. Arafat Ahmed Bhuiyan,  
Associate professor  
MPE Dept., IUT, Board Bazar, Gazipur-1704, Bangladesh

3.  (Examiner -2)  
Dr. Mohammad Monjurul Ehsan  
Associate Professor  
MPE Dept., IUT, Board Bazar, Gazipur-1704, Bangladesh.

## **Acknowledgement**

To the Almighty Allah, to whom we humbly submit ourselves, be all glory and thanks for blessing me with the skills and resources necessary to execute this enormous task within the allotted time. It would have been a far tougher task without His divine help, direction, and protection. I want to thank everyone who had a vital role in making this thesis project a reality and convey my deepest gratitude and admiration for their efforts. Their constant encouragement, direction, and oversight have been crucial throughout every step of this challenging trip. First and foremost, I owe a great deal of gratitude to my respected thesis supervisors, Dr. Arafat Ahmed Bhuiyan, Associate Professor, Department of Mechanical & Production Engineering, IUT and Dr. Md. Rezwanul Karim, Associate Professor, Department of Mechanical & Production Engineering, IUT Their extraordinary dedication, unflinching faith in my talent, and depth of knowledge have been instrumental in molding the results of my investigation. Their perceptive comments, helpful criticism, and careful scrutiny have inspired me to keep improving. Their guidance has helped me develop as researcher and as people, establishing in me a strong work ethic and a commitment to excellence. Their foresightful leadership and unflinching backing have paved the way for me, propelling me to overcome challenges and push the boundaries of my field.

Furthermore, I would like to extend my deepest appreciation to my beloved family and friends, whose persistent support, patience, and faith in my skills have been an endless well of inspiration. Their uncompromising confidence in my abilities has strengthened my resolve, comforted me in times of difficulty, and served as a reminder of the value of unflinching backing. All of the people that helped me in any way with my thesis project have my deepest gratitude. Because of your thoughtful contributions and intellectual curiosity, my work has been greatly improved. Finally, I would like to express my gratitude to Dr. Arafat Ahmed Bhuiyan and Dr. Md. Rezwanul Karim, my respective supervisors and mentors, whose unyielding commitment and profound competence have molded me into a stronger researcher and learner. My gratitude to them exceeds the limits of language.

To my respected professors and everyone else who helped me finish this thesis, I pray that Allah showers His blessings upon you.

Naimul Islam

ID: 180011206

## Abstract

Concerns over climate change and the depletion of nonrenewable energy sources have contributed to the widespread use of solar power. Solar energy is a renewable and environmentally friendly energy source since it can be converted directly into electricity using photovoltaic panels made of semiconducting materials. The production of heat energy from sun irradiation significantly reduces the efficiency of solar panels. In practice, for every 1°C increase in temperature, solar panel efficiency can drop by 0.4% to 0.65%. As a result, the panel's overall performance and electricity-generating capacity might drop. Adding a collector to the solar panel and extracting the heat with a working fluid is one solution to the problem of solar panels losing efficiency owing to thermal energy production. By reducing their thermal energy, the overall efficiency of solar panels can be improved with this method. In this study, the bottom of the PV panel is cooled using a photovoltaic thermal (PVT) collector. This technique improved the panel's heat management and boosted its performance. A numerical simulation of a PV panel coupled with a PVT collector using water and Fe<sub>3</sub>O<sub>4</sub> nanofluid as cooling medium was carried out in the software Ansys Fluent. The simulation was run with solar irradiation between 300 and 1100W/m<sup>2</sup>, and the nanofluid was used at different volume percentages. The study found that combining the use of water and Fe<sub>3</sub>O<sub>4</sub> nanofluid coolant significantly reduced the thermal energy produced by the PV panel, leading to an increase in overall efficiency. This finding proves the feasibility of using a cooling medium to improve solar panels' performance. The study simulated a variety of flow rates, solar irradiation, and volume concentrations. An efficiency of 12.5%-13.6 % was found for the solar cell, which is a significant increase over the 2.3% efficiency of a PV panel without a cooling mechanism. These findings suggest that increasing solar panel efficiency by using a nanofluid-based cooling technology is achievable.

**Keywords:** Photovoltaic thermal, Numerical simulation, Nanofluid, Fe<sub>3</sub>O<sub>4</sub>, Ansys Fluent, thermal cooling, thermal collector, efficiency.

## Nomenclatures

$A$	Surface area of pv panel [ $m^2$ ]
$E$	Energy [J]
$C_p$	Specific heat [ $J/kg^\circ C$ ]
$I$	Current [Ampere]
FF	Fill Factor
$h$	Coefficient of convection [ $W/m^2 \text{ }^\circ C$ ]
Ir <sub>ad</sub>	Solar radiation [ $W/m^2$ ]
I <sub>sc</sub>	Short circuit current [Ampere]
$k$	Conduction coefficient [ $W/m^\circ C$ ]
PMPP	Maximum output power [W]
V <sub>oc</sub>	Open circuit voltage [V]
PMPP(REF)	Maximum output power at reference temperature [W]
TC	Temperature coefficient of solar panel
$R$	Resistance [ $\Omega$ ]
$\mu$	Viscosity [kg/ms]
$\alpha$	Thermal diffusivity
$\rho$	Density [ $kg/m^3$ ]
$v$	Volume [ $m^3$ ]
$V$	Voltage [V]
$\rho_{nf}$	Density of nanofluid [ $kg/m^3$ ]
$\varphi$	Volume fraction of nanofluid

## Table of Contents

Candidate's Declaration.....	2
Acknowledgement .....	4
Abstract.....	5
Nomenclature.....	6
Chapter 1: Introduction.....	10
1.1 Background of the study: .....	10
1.2 Objectives of the study: .....	11
1.3 Structure of the thesis: .....	11
Chapter 2: Literature Review.....	12
Chapter 3: Description of the model.....	15
Chapter 4: Computational methodology.....	18
4.1: Governing Equation.....	19
4.2: Mesh .....	20
Chapter 5: Results & Discussion .....	21
Chapter 6: Conclusion.....	37
References.....	39

## List of Figures

Figure 1: Numerical modeling of the photovoltaic panel with the collector .....	15
Figure 2: Computational domain for thermal photovoltaic collector .....	16
Figure 3: Computational model of the 5 layers of the photovoltaic panel.....	17
Figure 4: Body sizing in the PV panel and stainless steel collector .....	18
Figure 5: Body sizing of 1.5mm of the photovoltaic panel along with the collector .....	20
Figure 6: Inflation mesh in the fluid domain .....	21
Figure 7: PV panel without any cooling .....	21
Figure 8: Temperature contour of water flowing at 1L/min and pv panel.....	22
Figure 9: Temperature contour of water flowing at 5L/min and pv panel.....	23
Figure 10: Temperature contour of PV panel and the fluid domain with $Fe_3O_4$ ( $\varphi =$ 0.2)flowrate at 5L/min.....	24
Figure 11: Temperature contour of PV panel and the fluid domain with $Fe_3O_4$ ( $\varphi =$ 0.6)flowrate at 5L/min.....	25
Figure 12: Temperature contour of PV panel and the fluid domain with $Fe_3O_4$ ( $\varphi =$ 1)flowrate at 5L/min.....	26
Figure 13: Temperature contour of PV panel and the fluid domain with $Fe_3O_4$ ( $\varphi =$ 1.5)flowrate at 5L/min.....	27
Figure 14: Temperature contour of PV panel and the fluid domain with $Fe_3O_4$ ( $\varphi =$ 2)flowrate at 5L/min.....	28
Figure 15: Temperature contour of PV panel and the fluid domain with $Fe_3O_4$ ( $\varphi =$ 1.5)flowrate at 4L/min.....	29
Figure 16: Temperature contour of PV panel and the fluid domain with $Fe_3O_4$ ( $\varphi =$ 1.5)flowrate at 3L/min.....	30
Figure 17: Temperature contour of PV panel and the fluid domain with $Fe_3O_4$ ( $\varphi =$ 1.5)flowrate at 2L/min.....	31
Figure 18: Temperature contour of PV panel and the fluid domain with $Fe_3O_4$ ( $\varphi =$ 1.5)flowrate at 1L/min.....	32
Figure 19: Temperature contour of PV panel and the fluid domain with $Fe_3O_4$ ( $\varphi =$ 1.5)flowrate at 5L/min, Heat flux =900W/m <sup>2</sup> .....	33
Figure 19: Temperature contour of PV panel and the fluid domain with $Fe_3O_4$ ( $\varphi =$ 1.5)flowrate at 5L/min, Heat flux =700W/m <sup>2</sup> .....	34



Figure 19: Temperature contour of PV panel and the fluid domain with Fe <sub>3</sub> O <sub>4</sub> ( $\varphi = 1.5$ )flowrate at 5L/min, Heat flux =500W/m <sup>2</sup> .....	35
Figure 19: Temperature contour of PV panel and the fluid domain with Fe <sub>3</sub> O <sub>4</sub> ( $\varphi = 1.5$ )flowrate at 5L/min, Heat flux =300W/m <sup>2</sup> .....	36

### **List of Tables**

Table 1: Working fluid properties .....	16
Table 2: Photovoltaic solar cell characteristics .....	17
Table 3: Compiled results of all the numerical simulation .....	36

## Chapter 1: Introduction

### 1.1 Background of the study:

The rising demand for energy and the ever-increasing cost of fossil fuels make it clear that we need to switch to more sustainable energy sources as soon as possible. Renewable energy is a promising answer since it uses sustainable and natural resources like the sun, the wind, the water, and the earth's geothermal and biomass systems. The sun provides the most readily available source of energy, and it may be captured through a number of different methods, the most common of which is photovoltaic systems. Solar power, for example, is a sustainable energy source that can help reduce our dependency on fossil fuels while simultaneously lessening the impact of climate change caused by human-caused greenhouse gas emissions. The potential for improvement of solar systems is the greatest among the several renewable energy options now available. Silicon solar cells and other doped structures constructed of silicon-phosphorus or silicon-boron convert solar energy to electrical energy when exposed to sunshine. Electrons in the silicon are displaced and excited when photons from the sun hit the cell, creating an electric current. Photovoltaic technology has the potential to become an increasingly attractive choice for the generation of renewable energy as long as research and development into the field is maintained. The ability of photovoltaic systems to convert dispersed sun irradiation gives them an edge over other solar cell variations. The efficiency of the system is diminished, however, by the heat energy produced by the solar cells' inefficiency [1]. When exposed to direct sunlight, photovoltaic (PV) panels generate heat that slows the flow of electrons, increasing resistance and reducing efficiency. An integrated collector system at the panel's base may remove the heat created by the sun's rays and restore the panel's original efficiency by bringing down the temperature. When the temperature of the panel rises by 1°C, its efficiency drops by 0.45% to 0.65%. [2]. A cooling system is one solution to the problem of PV panels overheating that might be considered. Hybrid solutions that integrate the PV panel with a cooling system have been developed to boost efficiency even further. The photovoltaic (PV) panel is an integral part of the hybrid system and comes in a wide range of sizes and designs to accommodate a wide range of needs. This approach provides a reasonable means of improving solar panel efficiency and advancing green energy [3].

## **1.2 Objectives of the study:**

The objective of this research is to use numerical simulation to explore and analyze the possible advantages and performance boost of employing  $\text{Fe}_3\text{O}_4$  nanofluid in a photovoltaic thermal (PVT) system. Firstly, the purpose of this study is to conduct a comprehensive literature review of photovoltaic thermal systems,  $\text{Fe}_3\text{O}_4$  nanofluids, and their combinations to better understand the present level of research on these topics. Secondly, the thermal conductivity, viscosity, and optical characteristics of  $\text{Fe}_3\text{O}_4$  nanofluid will be studied to see how they affect the PVT system's overall efficiency. In addition, to create a simulation model using numerical methods, taking into account the specifics of the PVT system and the  $\text{Fe}_3\text{O}_4$  nanofluid in which it operates. This model needs to take into account the system's thermal, hydrodynamic, and electrical dynamics. Thirdly, to compare the PVT system's efficiency when using  $\text{Fe}_3\text{O}_4$  nanofluid and when not, use a numerical simulation model. Evaluate the outcomes in terms of heat transfer improvement, electrical efficiency, and system performance as a whole. Determine the ideal circumstances for maximizing the performance of the PVT system using  $\text{Fe}_3\text{O}_4$  nanofluid by exploring various optimization tactics such as nanoparticle concentration, flow rate, and design parameters. Verify the accuracy of the numerical simulation by comparing the results to those from experiments or other sources. By focusing on these goals, the thesis paper can provide researchers, engineers, and policymakers with useful insights into the application of  $\text{Fe}_3\text{O}_4$  nanofluid in photovoltaic thermal systems.

## **1.3 Structure of the thesis:**

This thesis aims to accomplish thermal cooling of a photovoltaic (PV) panel using water and  $\text{Fe}_3\text{O}_4$  nanofluid as the working fluid, which will flow through the collector connected to the bottom surface of the PV panel. In chapter 1, the introduction of the thesis has been written i.e, background of the study, objectives of the study as well as the present scope of the study. The reason of choosing the specific nanofluid in the project has been described as well as the present scenario of energy sources has been described. In the chapter 2, a literature review of numerous photovoltaic panel cooling methods is presented. The present advancement of photovoltaic thermal systems in the literature was elaborately explained. In chapter 3, the model's geometry, dimensions, and nanofluid analysis are discussed. The numerical modelling as well as the simulation data were explained in this chapter. In chapter 4, the computational methodology is described in depth, followed by the presentation of results and discussion of the simulations in chapter 5 of the multiple simulations that were done in the paper, and lastly the conclusion is discussed in section 6.

## Chapter 2: Literature Review

A hybrid photovoltaic thermal (PVT) system's collector is built to maximize the simultaneous generation of thermal and electrical energy. As a result, PVT systems are an attractive option for improving the effectiveness of solar panels. [4]. The generated heat is typically collected by a cooling medium placed beneath the PV panel, and a steady flow of coolant keeps the internal temperature of the PV panel low. Next, convective heat transfer ensures the medium being cooled [5]. There are two aspects of the collector system that must be taken into account while constructing a hybrid PVT system. Before the heat from the PV panel can be transferred to the working fluid, the collector needs to have a high thermal conductivity. Second, it needs to be easily welded to the PV panel's bottom. The working fluid's collected heat can be employed to create thermal energy, dissipated in a heat exchanger, or discharged into the environment in some other way. The collector system then reuses the working fluid [6].

The effectiveness of a PV panel can be improved greatly by the addition of cooling solutions. Several different methods of cooling hybrid photovoltaic systems have been reported. Photovoltaic floating systems using water sprinklers were, for instance, conceived and built by R. Cazzaniga et al. By avoiding overheating, the panels last longer and produce more power [7]. In order to increase the overall power production, H. Hashim et al. used a thermoelectric generator to recuperate the excess heat produced by the solar cell. [8]. Popovici et al. created a computational model to lower the temperature of photovoltaic panels using air-cooled heat sinks. Different ribcage-to-base-plate angles were tested in their study [9].

To evaluate the effectiveness of a thermoelectric module (TEM) mounted on the back of a photovoltaic module (PV module), Aarti et al. created a mathematical model [10]. The TEM is meant to soak up the infrared radiation given off by the PV module. In order to control the working temperature of solar PV cells and prevent them from overheating, Shuang Ying Wu et al. proposed a heat pipe hybrid PV/T system [11]. The suggested technology effectively cools the PV cells by using a wick heat pipe to isothermally absorb the excess heat produced by the PV cells. This approach makes it easier to control the temperature and boosts the system's efficiency. The numerous solar flat plate PV/T technologies were summarized in a nutshell by Michael et al. [12], including their efficiency, prospective applications, benefits, limits, and topics for further research. Mingke et al. have presented two different heat pipe-based PV/T hybrid systems. The wire-meshed heat pipe PV/T system is only 51.5% efficient at 32 degrees Celsius, while the wickless heat pipe system is 52.8% efficient [13]. An array of flat plate solar collectors, a heat exchanger, two storage tanks, and connected pipelines were

used in the study by Sula and colleagues to determine the optimum pump flow rate for forced circulation solar water heating systems. The goal of their study was to find the optimal flow rate for the circulating fluid in order to boost the efficiency of the solar water heating system. Tonui et al. proposed enhancing heat transmission in air-cooled PV/T solar collectors by dangling a thin, flat metallic sheet or fins along the back wall of an air duct [14]. The goal was to increase the PV panel's overall efficiency. Saeed et al. investigated the effect of using various-sized copper tubes for cooling solar panels. The results of their studies have improved both thermal and general effectiveness. In [16], Govind et al. tested how well a nanofluid containing copper oxide may function as a thermal absorber in a photovoltaic thermal (PVT) system. An unglazed PVT system with a serpentine coil sheet and tube thermal absorber was investigated, and its electrical and thermal performance was assessed. The effectiveness of a photovoltaic thermal (PVT) panel was studied by Aghakhani et al. [17], who installed a copper pipe system for water cooling and fans for air conditioning underneath the panel. In order to get consistent temperatures across their solar panels, Fahad et al. ran an experiment using heat pipes and liquid immersion cooling [18]. The results showed a significant drop in temperature, with decreases of 48%, 25%, and 21% compared to passively chilled PV panels. [19]. Kadir et al. came up with a new cooler design and tested and analyzed how it affected the efficiency of a PVT system. When subjected to 900 W/m<sup>2</sup> of radiation, this layout showed a 4.67 percentage increase in electrical efficiency. The research found that the innovative cooler design boosted the efficiency of the PVT system. [20].

Two evaporators and two condensers were used in the solar ejector vapor compression refrigeration cycle studied by Ahmad et al., who looked at how to improve the cycle's efficiency by employing a photovoltaic thermal collector. Comparing R290 and R134a as evaporators, they found that R290 had a COP of 3 and a solar cooling efficiency of 4.8%, respectively [21]. Chen et al. investigated a novel cooling system that uses switchable film insulation and photovoltaic-thermal (PVT) collectors to transition between diurnal and nighttime modes. Switchable film insulation was shown to boost annual total energy yield by 10- 32% by reducing heat loss and optimizing system performance. [22]. The best settings for applying air-assisted water spray to the surface of PV panels were determined after Faruk Yesildal and colleagues ran 32 experiments. The purpose of this research was to compare the effects of spraying time, nozzle air flow rate, and nozzle to panel distance across three different intensities. [23]. An new solar thermal collector that can store heat and cold throughout the day and night has been proposed by Miao et al. Heat can only be collected with the conventional

glazed Flat Plate Solar Collector (FPSC) during the day. [24].

Five solar panels were used in an experiment by Talib et al. to see what would happen if titanium oxide nanofluid was added to the cooling fluid in a two-pass circulation system at varying concentrations. The research was conducted with the hope of improving the panel's performance by decreasing its operating temperature. Compared to utilizing only water or an uncooled panel, it was shown that adding nanofluid enhanced the heat transfer rate and decreased the surface temperature of the panel. [25]. A unique photovoltaic thermal module utilizing multiple baffles and nanofluids was proposed by M. Ahmedinejad and colleagues. Numerical performance evaluations were conducted on a variety of systems, such as the photovoltaic (PV) module, the basic channel collector PVT module, and the baffled channel collector PVT module, with each system operating with water, CuO/water nanofluid, and CNT/water nanofluid, respectively. The BPVTM/CuO and BPVTM/CNT modules outperformed the SPVTM/water system in terms of thermal power generation (9.46%), electrical power generation (2.12%), and reduction of solar cell temperature (13.88%), respectively. [26].

Particular attention will be given to the  $\text{Fe}_3\text{O}_4$  nanofluid because of the promising effects it may have on improving the efficiency of photovoltaic thermal systems. The scope will not include other nanofluids. In order to learn more about how  $\text{Fe}_3\text{O}_4$  nanofluid can be used in a photovoltaic thermal system, this study will mostly rely on numerical modeling methods. The research will not include any experimental work or field testing. This research will focus on one particular setup for a photovoltaic thermal system, taking into account its configuration's design factors such channel dimensions, fluid flow rates, and nanofluid concentration. Within bounds, it is possible to experiment with different configurations of the system to measure how they affect performance. The efficiency of the photovoltaic thermal system with and without the use of  $\text{Fe}_3\text{O}_4$  nanofluid will be compared. The research will be honest about its shortcomings, such as the model's simplifications and assumptions.

### Chapter 3: Description of the model

In this study, water and  $\text{Fe}_3\text{O}_4$  nanofluid were used in a thermal photovoltaic collector system to cool the solar panels. The dimension of the solar panel is  $590\text{mm}\times 490\text{mm}\times 4.71\text{mm}$ . A tube with a rectangular cross section was secured to the underside of the solar panel, and it carried the working fluid. The collector's metal plate is 1 mm thick and 30 mm by 15 mm in size; it is used to absorb heat. The flow pattern in the collector can be either linear or rectangular. At the bottom of the panel, there are 10 collector channels that will carry the working fluid. Stainless steel was chosen for the collector because of its high strength, malleability, and thermal conductivity [27]. The solar panels' heat-absorbing capability is improved when  $\text{Fe}_3\text{O}_4$  nanofluids are used as the working fluid [28]. This study aimed to determine if adding  $\text{Fe}_3\text{O}_4$

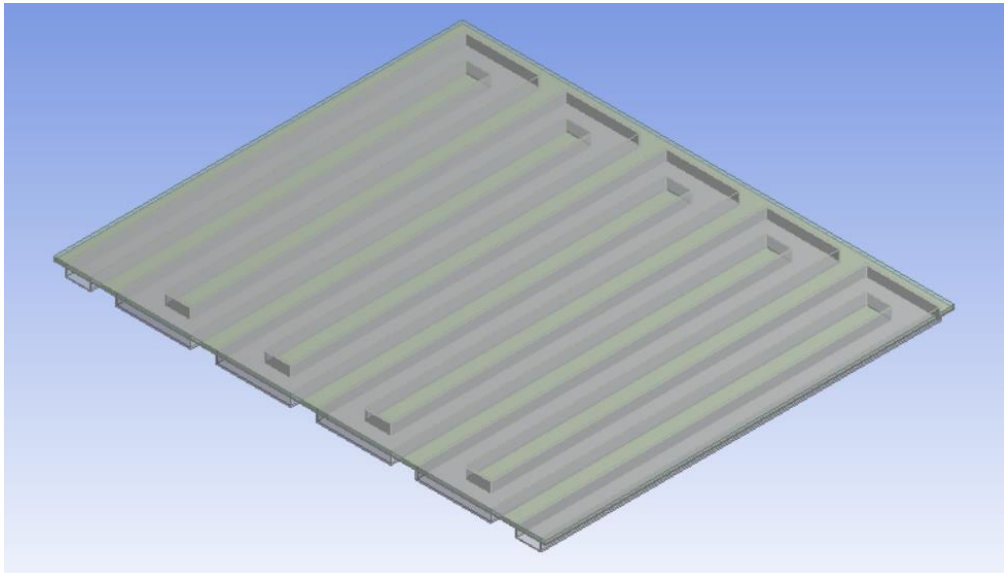


**Figure 1:** Numerical modeling of the photovoltaic panel with the collector

nanofluids to the PVT collector system's solar panels increased heat absorption efficiency. It was suggested that using  $\text{Fe}_3\text{O}_4$  nanofluids as the working fluid in place of pure water will increase the electrical efficiency of PV panels, especially when compared to PVT collector systems that do not have a cooling mechanism.  $\text{Fe}_3\text{O}_4$  nanofluids' properties are listed in Table 1. In figure 1, the numerical modeling of the photovoltaic panel with the collector has been illustrated. Here, we can see the thermal collector attached at the bottom of the 5 layered photovoltaic panel through which the thermal cooling is done by flowing water/nanofluid through the collector. For the numerical simulation modeling, we utilized the engineering simulation tool ANSYS Fluent and imported the geometry from solidworks.

Nanofluids are defined as a suspension of solid particles with an average size of less than 100 nm in an acidic liquid [30]. Increases in density, specific heat, dynamic viscosity, and thermal

conductivity are all effects of dissolving Fe<sub>3</sub>O<sub>4</sub> nanoparticles in sterile water [31]. In other words, the physical properties of purified water are enhanced by the addition of Fe<sub>3</sub>O<sub>4</sub> nanoparticles.

**Table 1:** Working fluid properties [29]

Fluid/Nanofluid	Density (kg/m <sup>3</sup> )	Thermal Conductivity (W/mK)	Specific Heat Capacity (J/kgK)
Water	1000	0.614	4180
Fe <sub>3</sub> O <sub>4</sub> ( $\varphi = 0.2$ )	1001.68	0.7167	4170.98
Fe <sub>3</sub> O <sub>4</sub> ( $\varphi = 0.6$ )	1020.95	0.77069	4156.9
Fe <sub>3</sub> O <sub>4</sub> ( $\varphi = 1$ )	1040.23	0.83456	4142.92
Fe <sub>3</sub> O <sub>4</sub> ( $\varphi = 1.5$ )	1064.31	0.8567	4125.38
Fe <sub>3</sub> O <sub>4</sub> ( $\varphi = 2$ )	1088.40	0.86978	4107.84

$\varphi = \text{Volume fraction}$

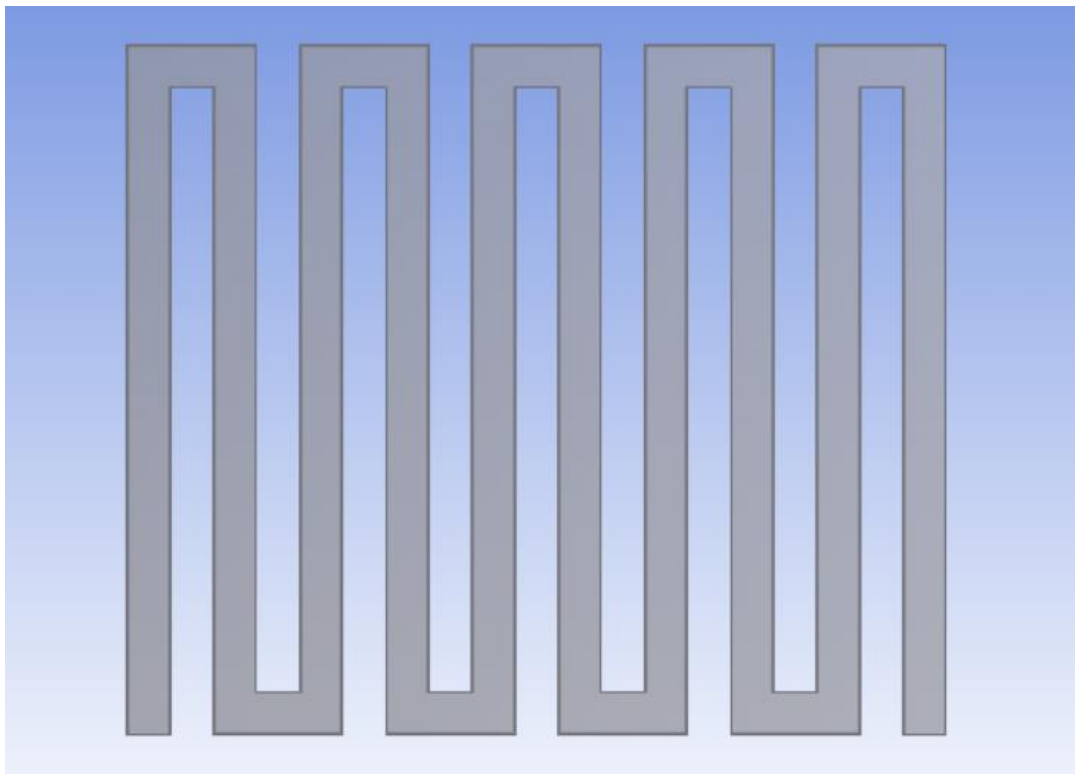


**Figure 2:** Computational domain for thermal photovoltaic collector.

To illustrate the pipe layout, consider Figure 2 where the computational domain for thermal photovoltaic collector has been mentioned. There are 10 channels in this collector of width 30mm each. The collector is attached at the bottom of the photovoltaic panel for the cooling purpose. In Table 2 we can see the PV features that were used. It was expected that solar panels cooled by PVT collectors would increase photovoltaic solar cell performance by decreasing the cell's working temperature.



**Table 2:** Photovoltaic solar cell characteristics [33].

Layers	Density (kg/m <sup>3</sup> )	Specific heat capacity (J/kgK)	Thermal conductivity (W/mK)	Thickness (mm)
Glass	2450	790	0.7	3.2
EVA	960	2090	0.311	0.5
PV cell	2330	677	130	0.21
EVA	960	2090	0.311	0.5
PVF	1200	1250	0.15	0.3

In order to anticipate the temperature distribution of photovoltaic cells and water collectors, the equation was numerically solved using a three-dimensional fluid dynamics simulation model. Since the top surface of the solar cell is the only one in contact with the heat flow, it serves as a representation of the boundary conditions. Heat convection and stagnation were, therefore, assumed to occur only in the solar cell's outside layer. Glass, EVA, PV cell, EVA, and PVF are the 5 layers that make up the solar panel, as shown in Fig. 2. The temperature was kept at 30 degrees Celsius during the entire experiment. Water coming into the system and water going out both experienced an absolute pressure of 1 bar.

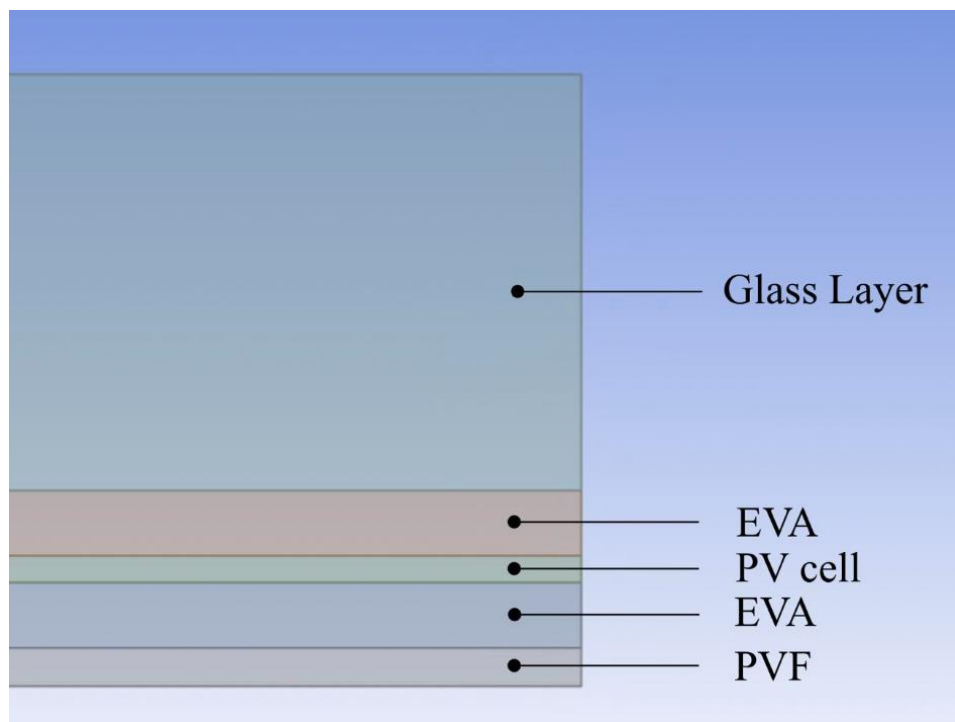


**Figure 3:** Computational model of the 5 layers of the photovoltaic panel

The heat transfer between the PV cell layer and the liquid was modeled and simulated using both the steady-state thermal software and the Fluent program. As an alternative to modeling, research into solar heat transfer is conducted in conjunction with heat fluxes that do not impact the coating of PV cells. The geometric model for the CFD analysis was made in Solidworks, and the meshing was done in ANSYS Meshing Software.

## Chapter 4: Computational methodology

Solidworks was initially used to create a model of the pv panel and collector separately. After that, meshing was completed using body sizes. Convective heat loss of  $6 \text{ W/m}^2\text{K}$  was utilized on all 5 lateral sides of the PV panel, including the bottom face, and a heat flux of  $1100 \text{ W/m}^2$  was employed on the top glass layer. In this manner, the grounded photovoltaic system was installed without the need for a cooling system.

Secondly, Solidworks was used to create the model of the pv and collector. After that, Ansys was given the geometry data. The PV/T system's geometry is depicted in Figure 1. Both the solids (body sizing) and fluid (inflation) were meshed (PV panel with collector: Nodes: 2945714 Elements: 4253960). From figure 4 we can see the body sizing in the PV panel and stainless steel collector. Then, the grounded pv panel's heat flux and convective heat loss values were adjusted during setup. In case of water an inlet mass flow rate of  $0.0833 \text{ kg/s}$  ( $5\text{L/min}$ ) was set. The intake mass flow rates were  $5\text{L/min}$ ,  $4\text{L/min}$ ,  $3\text{L/min}$ ,  $2\text{L/min}$ , and  $1\text{L/min}$  when using  $\text{Fe}_3\text{O}_4$  as the working fluid.

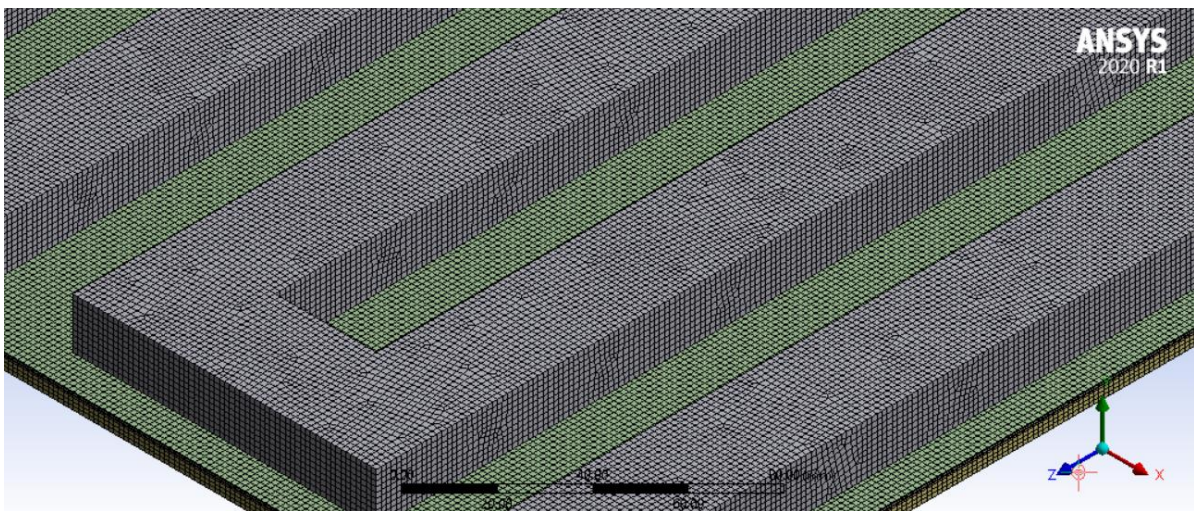


**Figure 4:** Body sizing in the PV panel and stainless steel collector.

Here, heat flux was varied from  $1100 \text{ W/m}^2$  to  $900 \text{ W/m}^2$  to  $700 \text{ W/m}^2$  to  $500 \text{ W/m}^2$  to  $300 \text{ W/m}^2$ . The top surface area of the PV panel is  $0.2891 \text{ m}^2$ . The collector benefits from SS316L's corrosion-resistant and ductile qualities. Prior to establishing the varied thermal characteristics of the nanofluids at different volume fractions, the density, thermal conductivity, and specific heat of all five pv panel layers, water, and stainless steel were fixed. The input and ambient temperatures are both  $303 \text{ degrees Kelvin}$ , and the outlet gauge pressure has been adjusted to zero. The residual was set at  $10^{-16}$ . Then the calculation was initiated.

#### 4.1 Governing Equation

The density of the nanofluid can be predicted in accordance with the mixing theory.

$$\rho_{nf} = (1 - \varphi)\rho_{bf} + \varphi\rho_{np} \quad (1)$$

Nanofluid specific heat at a given concentration can be determined using the formulae:

$$C_{p,nf} = \{(1 - \varphi)(\rho C_p)_{bf} + \varphi(\rho C_p)_{np}\} / \{(1 - \varphi)\rho_{bf} + \varphi\rho_{np}\} \quad (2)$$

The example below illustrates how to represent the empirical equation for thermal conductivity [35]:

$$k_{nf}(T) = k_{bf}(T) \cdot (a + b\varphi) \quad (3)$$

where  $a = 1.0191$  and  $b = 0.00352$  respectively.

PMPP is the point on a current-voltage (I-V) curve at which the solar PV devices generates the largest output i.e. the product of current flow (I) and voltage (V) is maximum. Theoretically, PMPP (Maximum power point) is calculated from temperature coefficient equation for maximum power point (MPP) tracking in photovoltaic systems [36].

$$PMPP(T) = PMPP(REF) \times [1 - TC \times (T - T_{REF})] \quad (4)$$

where,  $PMPP(T)$  is the maximum power point at temperature T,  $PMPP(REF)$  is the maximum power point at the reference temperature which is 25°C and  $TC$  is the temperature coefficient of the solar panel.

The reference PMPP can be found out by the following formula

$$\begin{aligned} PMPP(REF) &= I_{mp} \times V_{mp} \\ &= FF \times I_{sc} \times V_{oc} \quad [37, 38] \end{aligned} \quad (5)$$

Here, fill factor,  $FF = 0.686$  and  $I_{sc} = 2.87A$ ,  $V_{oc} = 22.9V$  and temperature coefficient of power,  $TC = 0.45\%$  per degree Celsius for the specific PV panel whose model is ‘YINGLI Solar JS50 polycrystalline 50 Wp (Watt peak)’ [39]

The power of incident light is calculated by the following formula [40]

$$P_{light} = I_{rad} \times A \quad (6)$$

where  $I_{rad}$  is the radiation intensity of the solar flux.  $A$  is the surface area of the solar panel

Electrical efficiency of the solar cell is calculated by the following formula

$$\eta = PMPP(T) / P_{light} \times 100\% \quad (7)$$

## 4.2 Mesh

Body sizing of 1.5mm were done in both the 5 layered photovoltaic panel as well as the stainless steel collector. Since the geometry is less than 1m in dimension along any of the axis, the mesh is dense compared with the geometry of the photovoltaic panel. In figure 5, the body mesh of the pv panel and the rectangular collector has been shown.

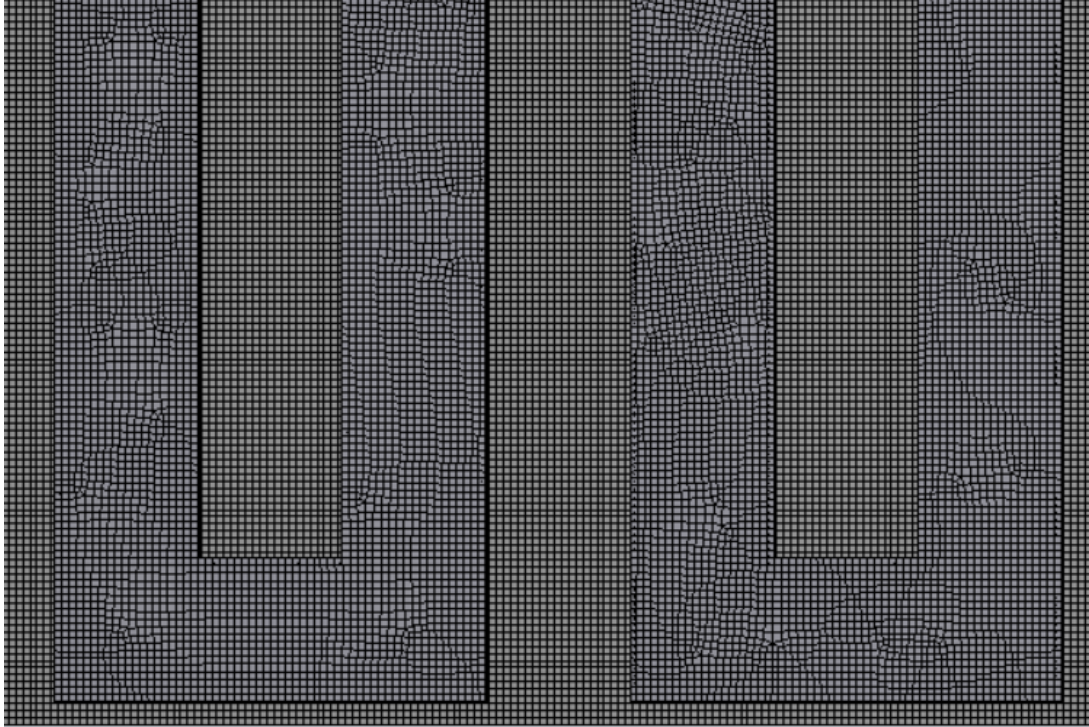


**Figure 5:** Body sizing of 1.5mm of the photovoltaic panel along with the collector

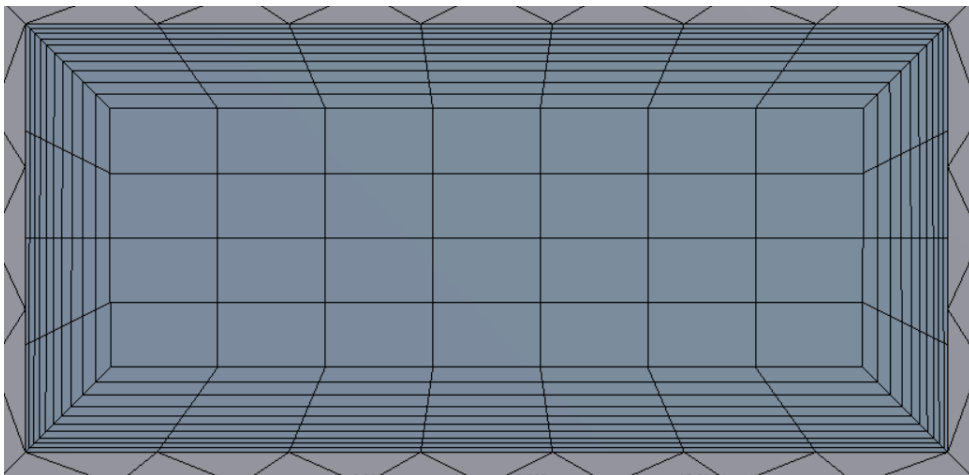


**Figure 6:** Inflation mesh in the fluid domain.

In figure 6, the inflation mesh done at the fluid domain is depicted. The boundary was set as the inner wall of the stainless steel. Maximum layers were set as 10 and the growth rate was set as 1.2.



## Chapter 5: Results & Discussion

In total 16 cases were studied under the simulation. The cases were considered based on different flowrates of water and nanofluid. Photovoltaic system without any cooling panel is one of the cases. Additionally, simulation were done at varying volume fractions of the nanofluid. In the last section, simulations were done at varying heat flux values. Therefore, the result section discusses the results of pv ground system i.e. photovoltaic panel without any cooling system, then water cooled pv panel, then nanofluid cooled pv panel at varying volume fractions, then at varying flowrates then at varying heat flux values.

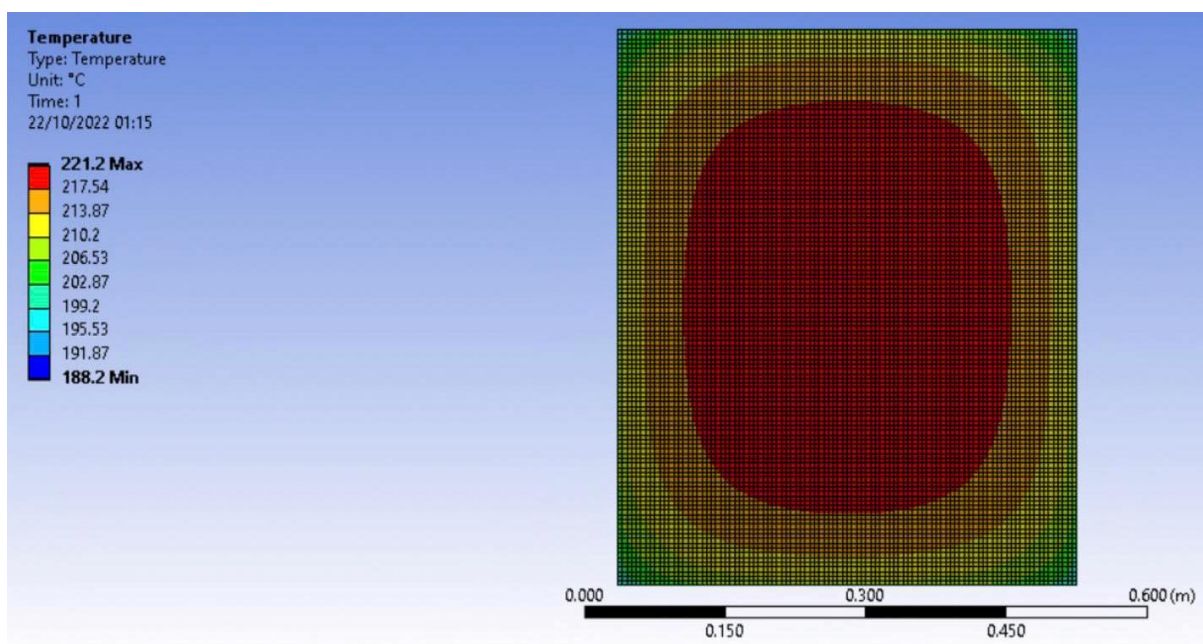


**Figure 7:** PV panel without any cooling

In figure 7, the temperature contour of the photovoltaic panel without any cooling system has been depicted. From here we can see that the central region's temperature is more than the side portions. The reason is due to convective heat loss of  $6 \text{ W/m}^2$  through the lateral walls. The area weighted average temperature for the PV ground system is  $210.73^\circ\text{C}$  at a heat flux value of  $1100 \text{ W/m}^2$ , with a maximum temperature of  $221.2^\circ\text{C}$  and a minimum temperature of  $188.2^\circ\text{C}$ . Without a cooling system, this PV panel has an efficiency of 2.32% and a PMPP value of 7.378W.

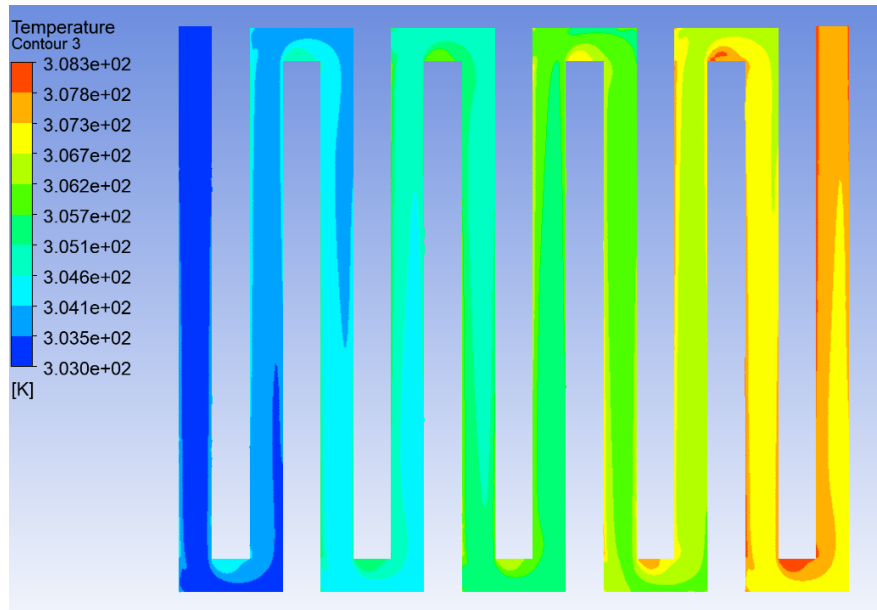


**Figure 8(a):** Temperature contour of water flowing at 1L/min

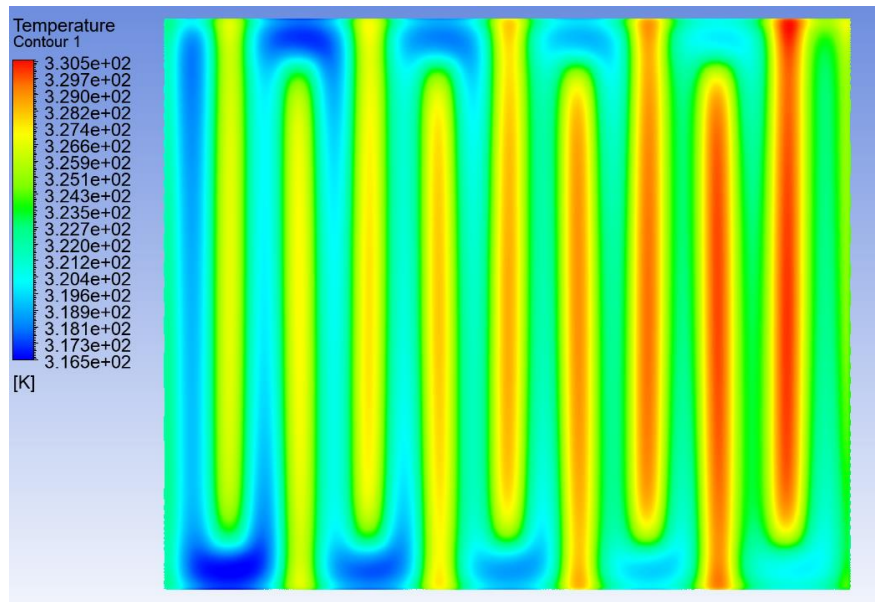


**Figure 8(b):** Temperature contour of PV panel where water flowrate is 1L/min

In figure 8(a) we can see the temperature contour of the fluid domain whereas in figure 8(b) we can see the temperature distribution in the photovoltaic panel. In the results of the simulation where the water was flowed at a flowrate of 1L/min and the heat flux as  $1100\text{W/m}^2$ . The PV panel reached a high of  $57.35\text{ }^\circ\text{C}$  and a low of  $43.35\text{ }^\circ\text{C}$  during the experiment. The area weighted average temperature was  $50.74\text{ }^\circ\text{C}$ . The calculated PMPP for this temperature is  $39.85\text{W}$  and the solar cell efficiency is calculated and obtained as  $12.53\%$ .

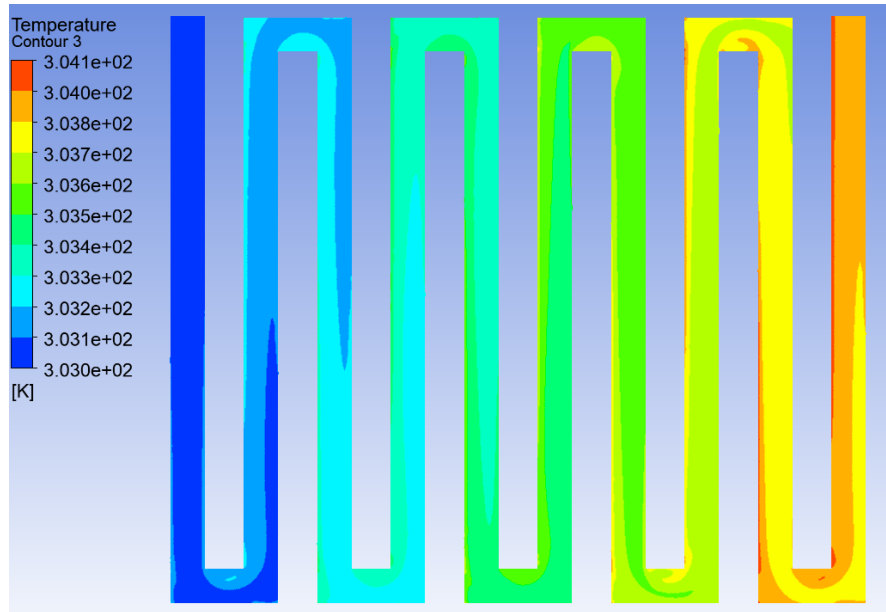


**Figure 9(a):** Temperature contour of water flowing at 5L/min

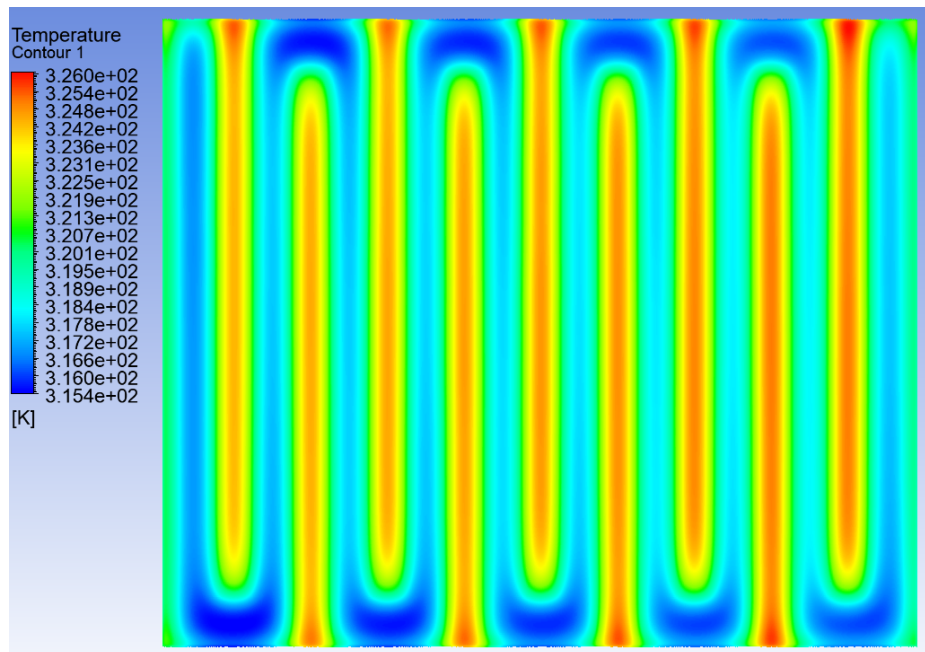


**Figure 9(b):** Temperature contour of PV panel with water flowrate of 5L/min

In figure 9(a) the temperature contour of the fluid domain passing through the collector whereas in figure 9(b) the temperature distribution in the photovoltaic panel has been depicted. In the results of the simulation where the water was flowed at a flowrate of 5L/min and the heat flux set as  $1100\text{W/m}^2$ , maximum temperature measured on the PV panel was  $53^\circ\text{C}$ , with a minimum of  $42.25^\circ\text{C}$ . The area weighted average temperature was  $47.33^\circ\text{C}$ . The calculated PMPP for this temperature is calculated as  $40.54\text{W}$  and thus the efficiency is found to be  $12.75\%$ .

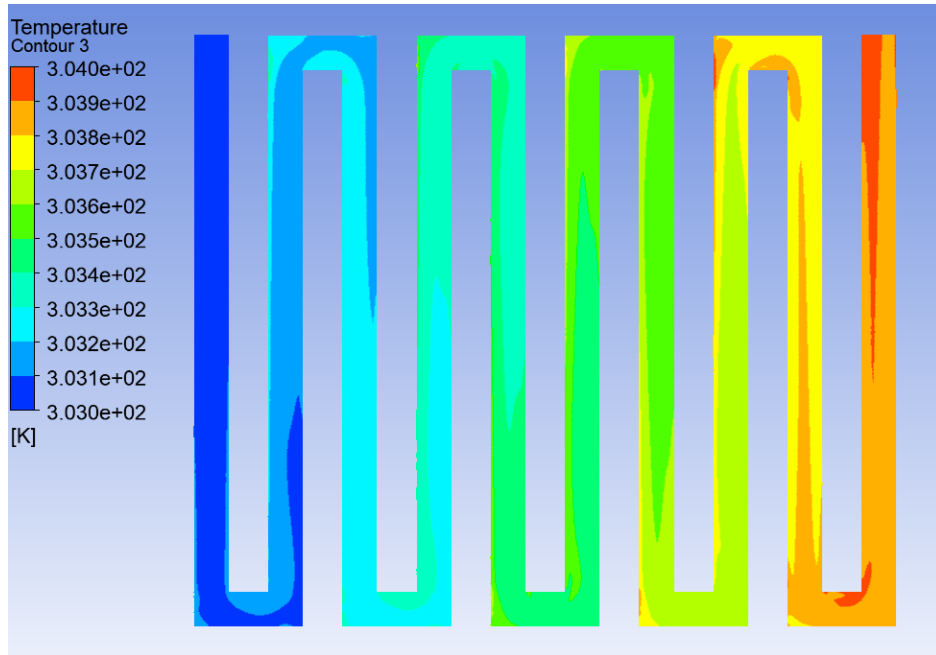


**Figure 10(a):** Temperature contour of  $\text{Fe}_3\text{O}_4$  ( $\phi = 0.2$ ) flowrate at 5L/min

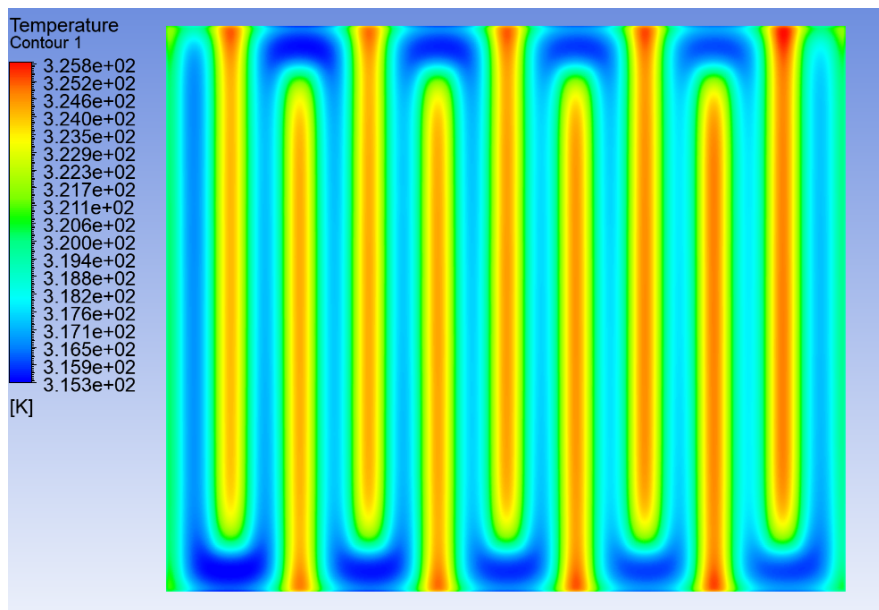


**Figure 10(b):** Temperature contour of PV panel with  $\text{Fe}_3\text{O}_4$  ( $\phi = 0.2$ ) flowrate at 5L/min

The temperature distribution of the fluid domain passing through the collector has been mentioned in the figure 10(a) whereas in the figure 10(b) the temperature contour of the photovoltaic panel has been depicted. In the results of this simulation of  $\text{Fe}_3\text{O}_4$  ( $\phi = 0.2$ ) flowing at 5L/min and the heat flux set at  $1100\text{W/m}^2$ . The PV panel reached  $52.65$  degrees Celsius at its hottest and dropped to  $42.15$  degrees Celsius at its coldest. The area weighted average temperature was  $47.11^\circ\text{C}$ . The calculated PMPP for this temperature is  $40.6\text{W}$  and the efficiency is  $12.77\%$ .



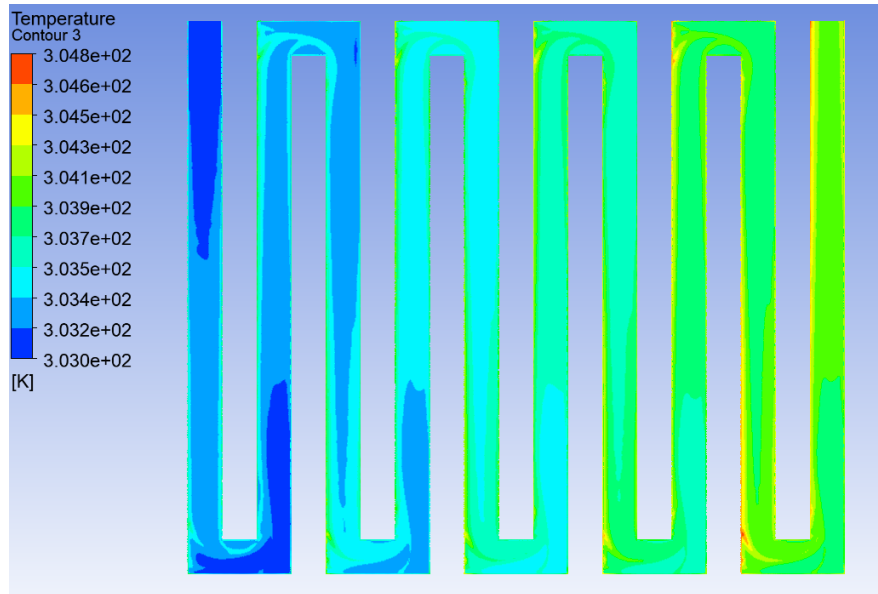


**Figure 11(a):** Temperature contour of  $\text{Fe}_3\text{O}_4$  ( $\varphi = 0.6$ ) flowrate at 5L/min

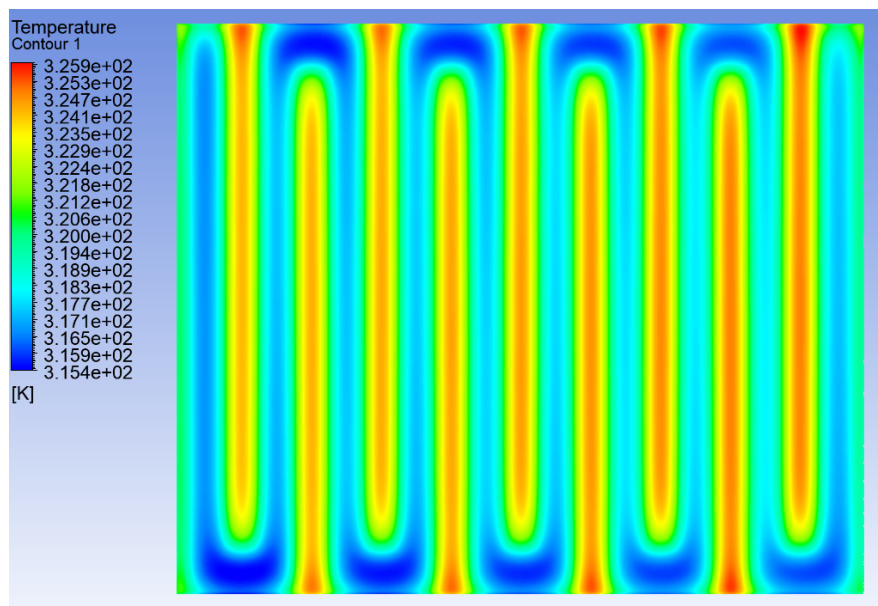


**Figure 11(b):** Temperature contour of PV panel with  $\text{Fe}_3\text{O}_4$  ( $\varphi = 0.6$ ) flowrate at 5L/min

The temperature distribution of the fluid domain passing through the collector has been mentioned in the figure 11(a) whereas in the figure 11(b) the temperature contour of the photovoltaic panel has been depicted. In the results of this simulation of  $\text{Fe}_3\text{O}_4$  ( $\varphi = 0.6$ ) flowing at 5L/min and the heat flux set at  $1100\text{W}/\text{m}^2$ . The PV panel reached  $52.75^\circ\text{C}$  at its hottest and dropped to  $42.25^\circ\text{C}$  at its coldest. The area weighted average temperature was  $47.17^\circ\text{C}$ . The calculated PMPP for this temperature is  $40.57\text{W}$  and the efficiency is  $12.75\%$ .

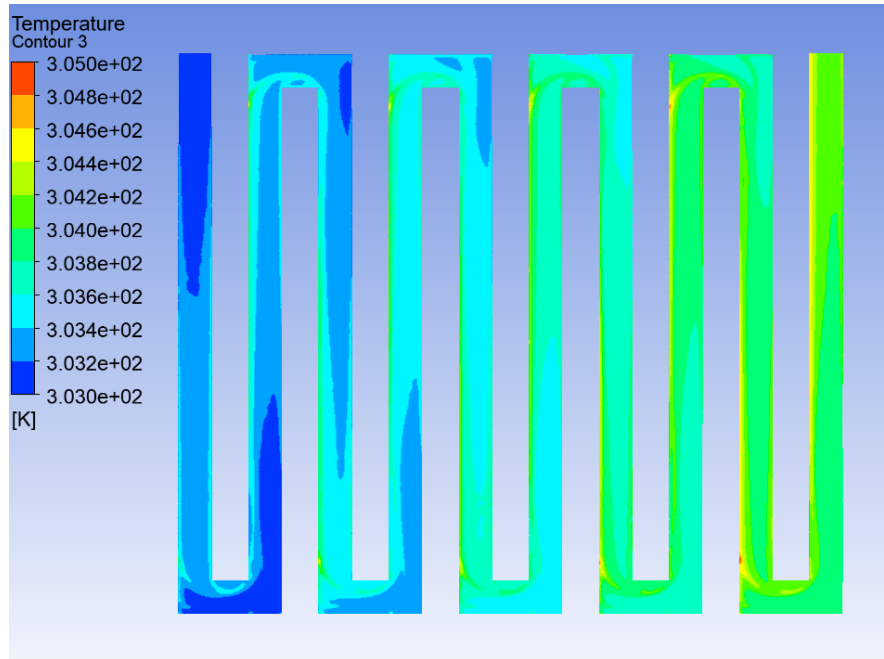


**Figure 12(a):** Temperature contour of  $\text{Fe}_3\text{O}_4$  ( $\varphi = 1$ ) flowrate at 5L/min

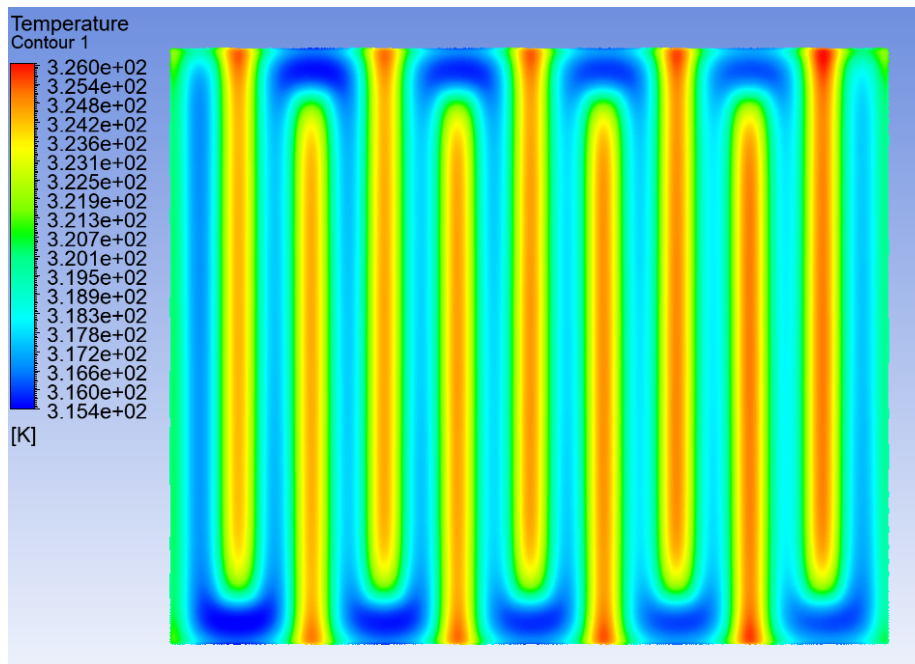


**Figure 12(b):** Temperature contour of PV panel with  $\text{Fe}_3\text{O}_4$  ( $\varphi = 1$ ) flowrate at 5L/min

The temperature distribution of the fluid domain passing through the collector has been mentioned in the figure 12(a) whereas in the figure 12(b) the temperature contour of the photovoltaic panel has been depicted. In the results of this simulation of  $\text{Fe}_3\text{O}_4$  ( $\varphi = 1$ ) flowing at 5L/min and the heat flux set at  $1100\text{W}/\text{m}^2$ . The PV panel reached a high of  $52.85^\circ\text{C}$  and a low of  $42.25^\circ\text{C}$ . The area weighted average temperature was  $47.31^\circ\text{C}$ . The calculated PMPP for this temperature is  $40.54\text{W}$  and the efficiency is  $12.75\%$ .

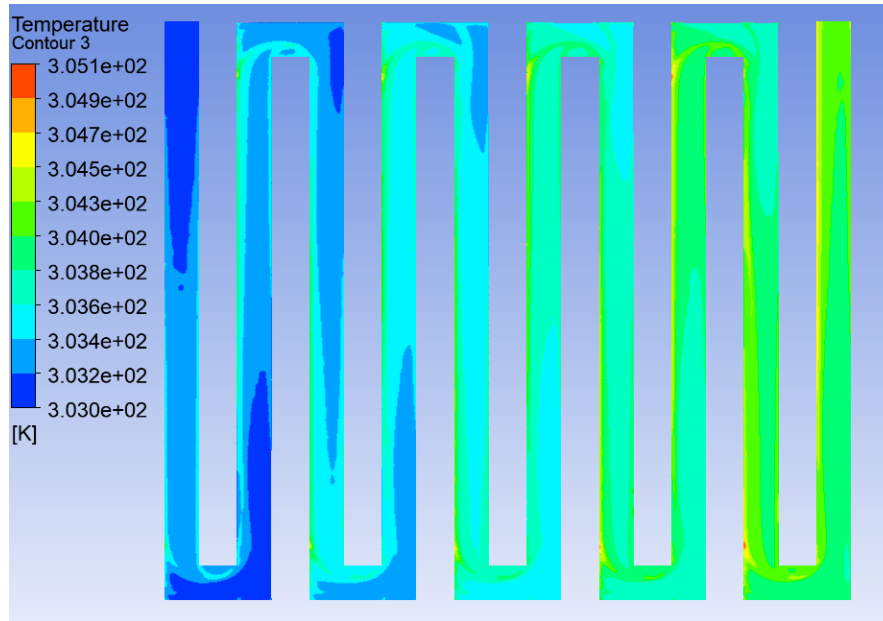


**Figure 13(a):** Temperature contour of  $\text{Fe}_3\text{O}_4$  ( $\phi = 1.5$ ) flowrate at 5L/min

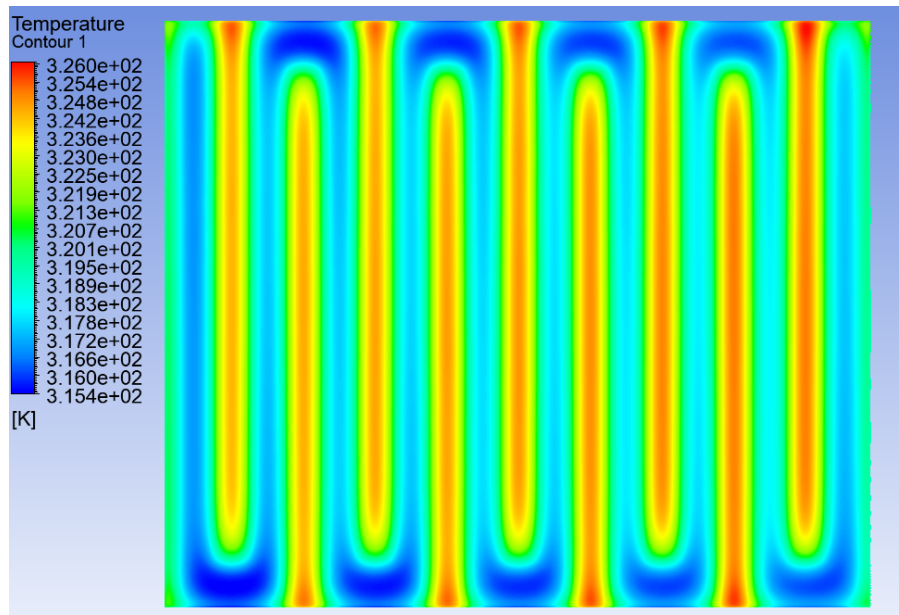


**Figure 13(b):** Temperature contour of PV panel with  $\text{Fe}_3\text{O}_4$  ( $\phi = 1.5$ ) flowrate at 5L/min

The temperature distribution of the fluid domain passing through the collector has been mentioned in the figure 13(a) whereas in the figure 13(b) the temperature contour of the photovoltaic panel has been depicted. In the results of this simulation of  $\text{Fe}_3\text{O}_4$  ( $\phi = 1.5$ ) flowing at 5L/min and the heat flux set at  $1100\text{W/m}^2$ . The PV panel reached  $52.85^\circ\text{C}$  at its hottest and dropped to  $42.25^\circ\text{C}$  at its coldest. The area weighted average temperature was  $47.25^\circ\text{C}$ . The calculated PMPP for this temperature is  $40.54\text{W}$  and the efficiency is  $12.75\%$ .

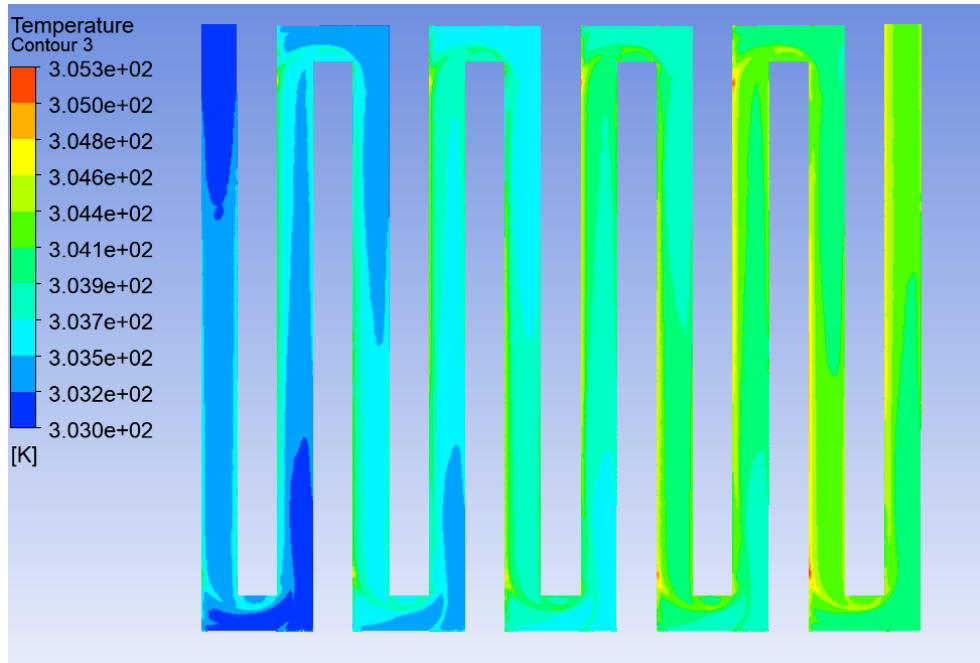


**Figure 14(a):** Temperature contour of  $\text{Fe}_3\text{O}_4$  ( $\varphi = 1.5$ ) flowrate at 4L/min

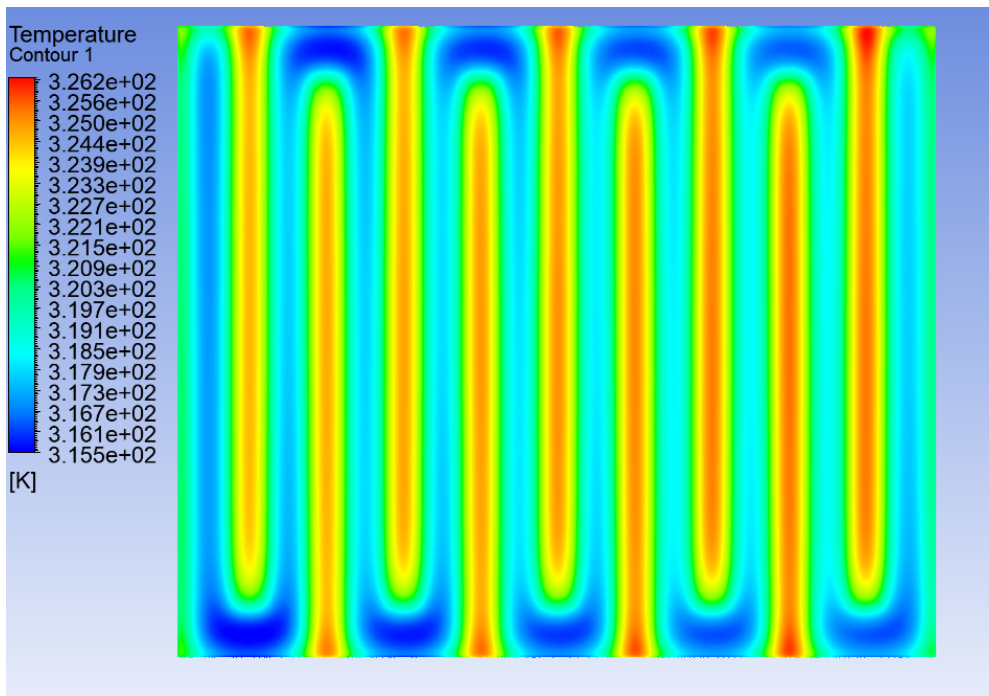


**Figure 14(b):** Temperature contour of PV panel with  $\text{Fe}_3\text{O}_4$  ( $\varphi = 1.5$ ) flowrate at 4L/min

The temperature distribution of the fluid domain passing through the collector has been mentioned in the figure 14(a) whereas in the figure 14(b) the temperature contour of the photovoltaic panel has been depicted. In the results of this simulation of  $\text{Fe}_3\text{O}_4$  ( $\varphi = 1.5$ ) flowing at 4L/min and the heat flux set at  $1100\text{W/m}^2$  The PV panel reached a high of  $53.05^\circ\text{C}$  and a low of  $42.35^\circ\text{C}$ . The area weighted average temperature was  $47.57^\circ\text{C}$ . The calculated PMPP for this temperature is  $40.48\text{W}$  and the efficiency is  $12.73\%$ .

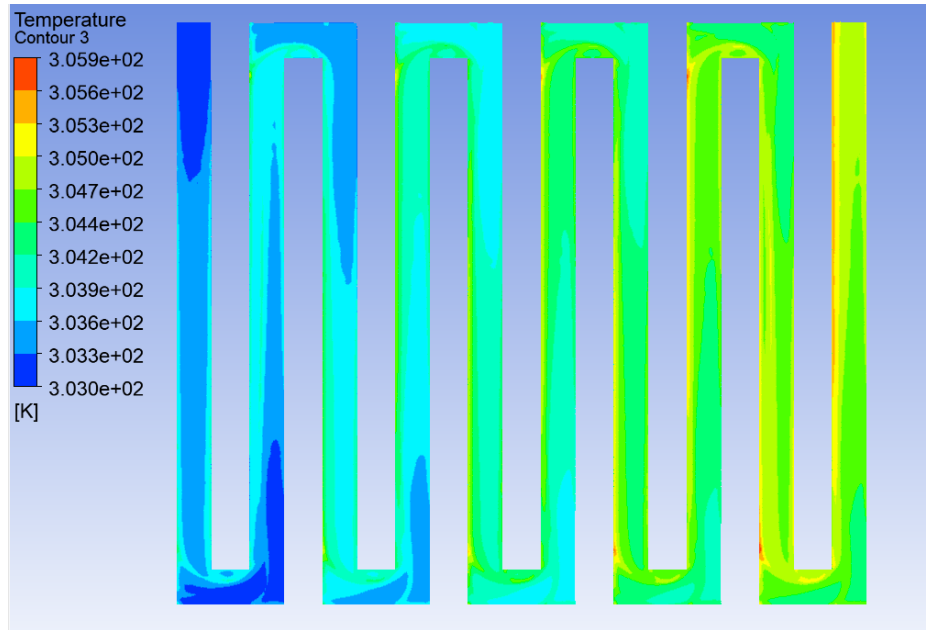


**Figure 15(a):** Temperature contour of  $\text{Fe}_3\text{O}_4$  ( $\varphi = 1.5$ ) flowrate at 3L/min

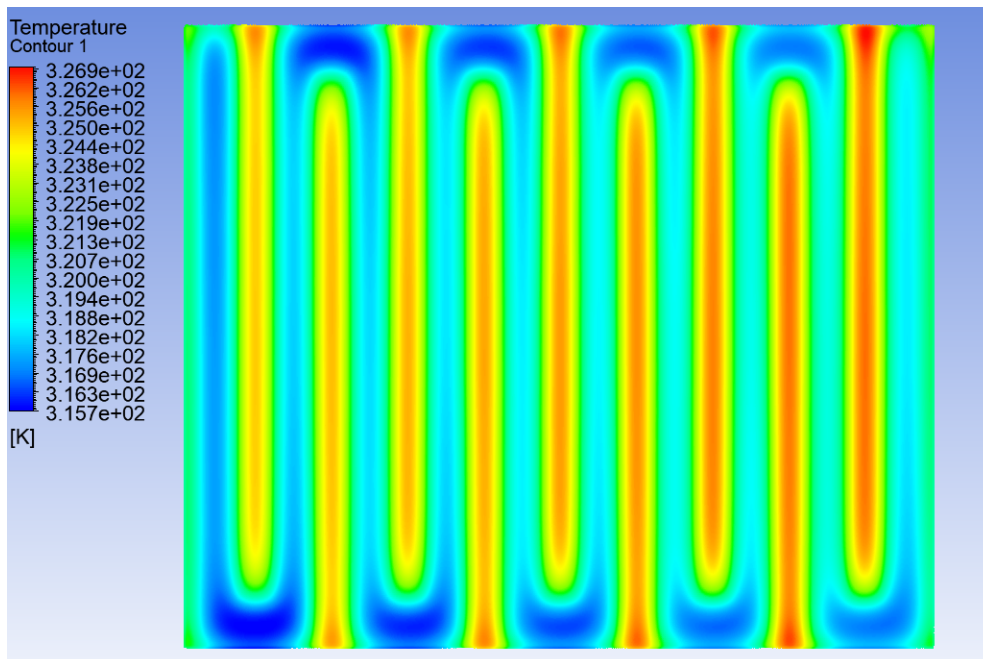


**Figure 15(b):** Temperature contour of PV panel with  $\text{Fe}_3\text{O}_4$  ( $\varphi = 1.5$ ) flowrate at 3L/min

The temperature distribution of the fluid domain passing through the collector has been mentioned in the figure 15(a) whereas in the figure 15(b) the temperature contour of the photovoltaic panel has been depicted. In the results of this simulation of  $\text{Fe}_3\text{O}_4$  ( $\varphi = 1.5$ ) flowing at 3L/min and the heat flux set at  $1100\text{W}/\text{m}^2$ . The PV panel's highest recorded temperature was  $53.75^\circ\text{C}$ , while its lowest recorded temperature was  $42.55^\circ\text{C}$ . The area weighted average temperature was  $48^\circ\text{C}$ . The calculated PMPP for this temperature is  $40.4\text{W}$  and the efficiency is  $12.7\%$

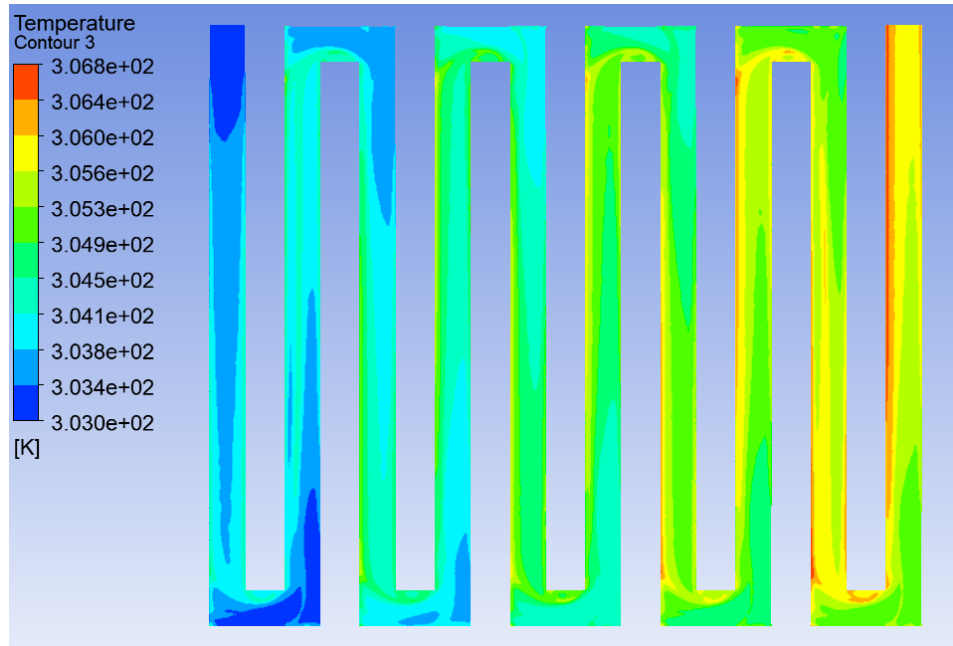


**Figure 16(a):** Temperature contour of  $\text{Fe}_3\text{O}_4$  ( $\varphi = 1.5$ ) flowrate at 2L/min

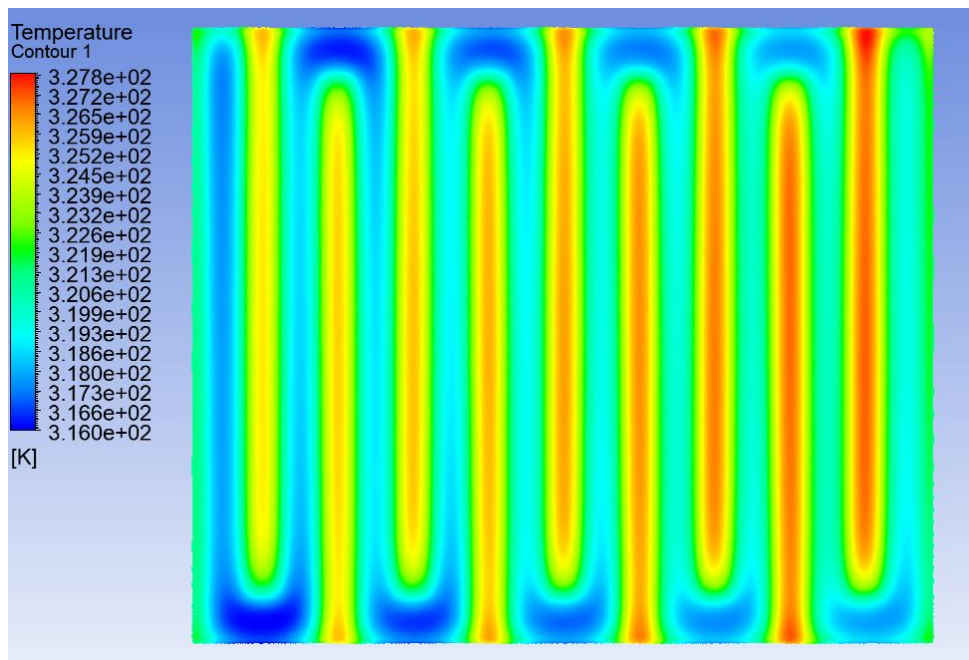


**Figure 16(b):** Temperature contour of PV panel with  $\text{Fe}_3\text{O}_4$  ( $\varphi = 1.5$ ) flowrate at 2L/min

In figure 16(a) the temperature contour of the fluid domain has been shown and in figure 16(b) the temperature contour of the photovoltaic panel has been shown. In the results of this simulation of  $\text{Fe}_3\text{O}_4$  ( $\varphi = 1.5$ ) flowing at 2L/min and the heat flux set at  $1100\text{W}/\text{m}^2$  The PV panel reached a high of  $54.65^\circ\text{C}$  and a low of  $42.85^\circ\text{C}$ . The area weighted average temperature was  $48.75^\circ\text{C}$ . The calculated PMPP for this temperature is  $40.25\text{W}$  and the efficiency is  $12.65\%$

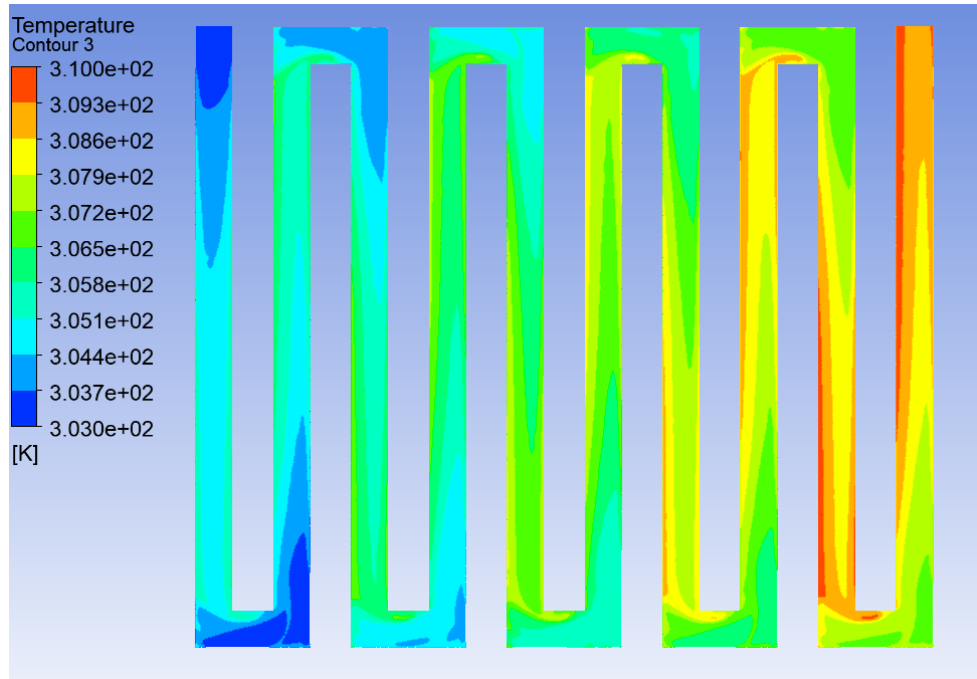


**Figure 17(a):** Temperature contour of  $\text{Fe}_3\text{O}_4$  ( $\varphi = 1.5$ ) flowrate at 1L/min

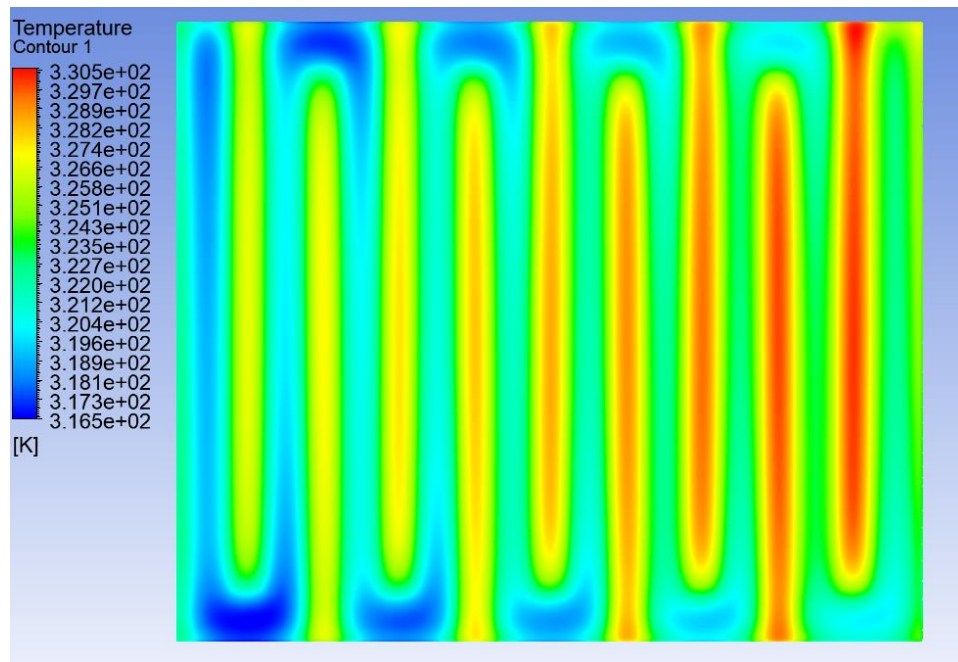


**Figure 17(b):** Temperature contour of PV panel with  $\text{Fe}_3\text{O}_4$  ( $\varphi = 1.5$ ) flowrate at 1L/min

In figure 17(a) the temperature contour of the fluid domain has been shown and in figure 17(b) the temperature contour of the photovoltaic panel has been shown. In the results of this simulation of  $\text{Fe}_3\text{O}_4$  ( $\varphi = 1.5$ ) flowing at 1L/min and the heat flux set at  $1100\text{W}/\text{m}^2$ . The PV panel reached a high of  $57.35\text{ }^\circ\text{C}$  and a low of  $43.35\text{ }^\circ\text{C}$ . The area weighted average temperature was  $50.75\text{ }^\circ\text{C}$ . The calculated PMPP for this temperature is  $39.84\text{W}$  and the efficiency is  $12.52\%$



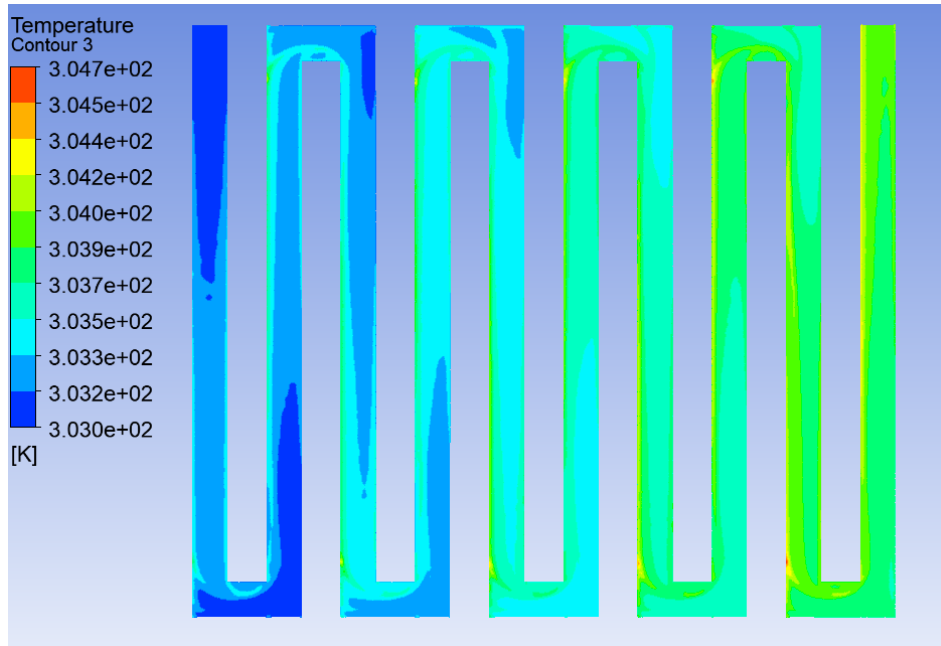


**Figure 18(a):** Temperature contour of  $\text{Fe}_3\text{O}_4$  ( $\phi = 1.5$ ) flowrate = 5L/min,  
heat flux =  $900\text{W/m}^2$

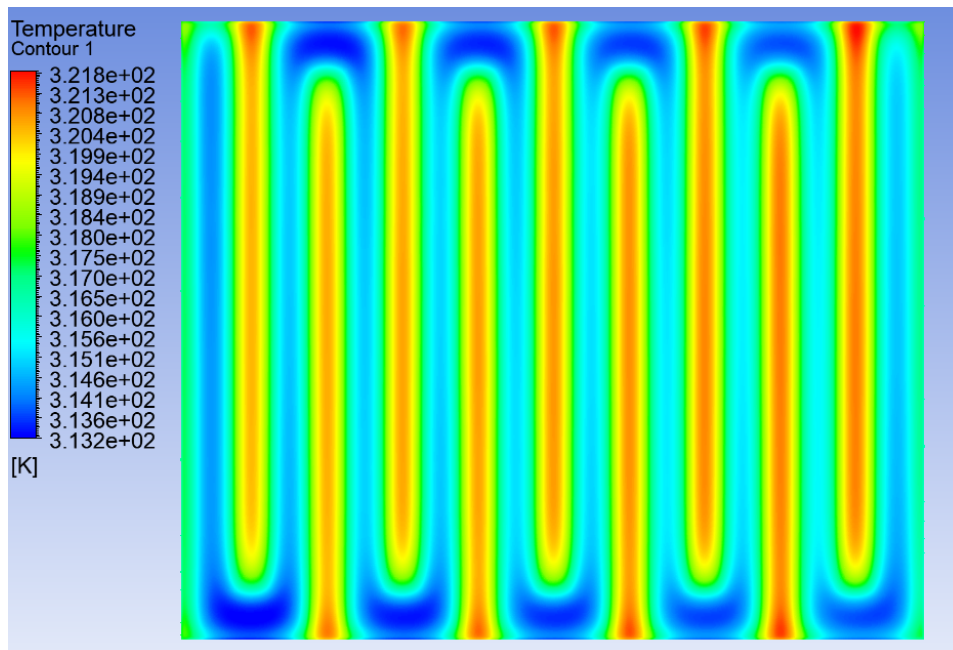


**Figure 18(b):** Temperature contour of PV panel with  $\text{Fe}_3\text{O}_4$  ( $\phi = 1.5$ ) flowrate at 5L/min,  
heat flux at  $900\text{W/m}^2$

In figure 18(a) the temperature contour of the fluid domain has been shown and in figure 18(b) the temperature contour of the photovoltaic panel has been shown. In the results of this simulation of  $\text{Fe}_3\text{O}_4$  ( $\phi = 1.5$ ) flowing at 5L/min and the heat flux set at  $900\text{W/m}^2$  The PV panel reached a high of  $48.65\text{ }^\circ\text{C}$  and a low of  $40.05\text{ }^\circ\text{C}$  over its simulation. The area weighted average temperature was  $44.14\text{ }^\circ\text{C}$ . The calculated PMPP for this temperature is  $41.185\text{W}$  and the efficiency is  $12.95\%$



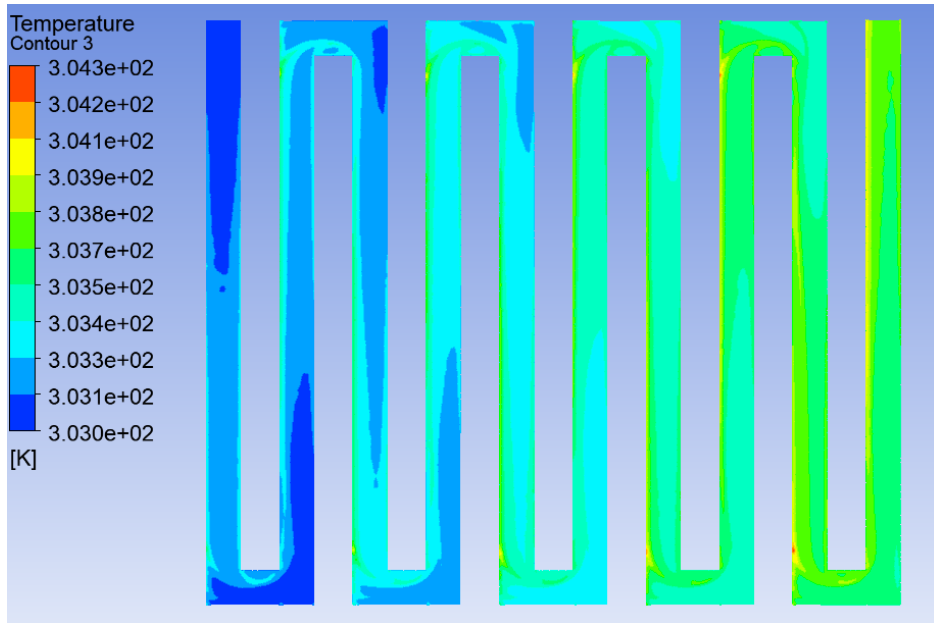


**Figure 19(a):** Temperature contour of  $\text{Fe}_3\text{O}_4$  ( $\phi = 1.5$ ) flowrate = 5L/min,  
heat flux =  $700\text{W/m}^2$

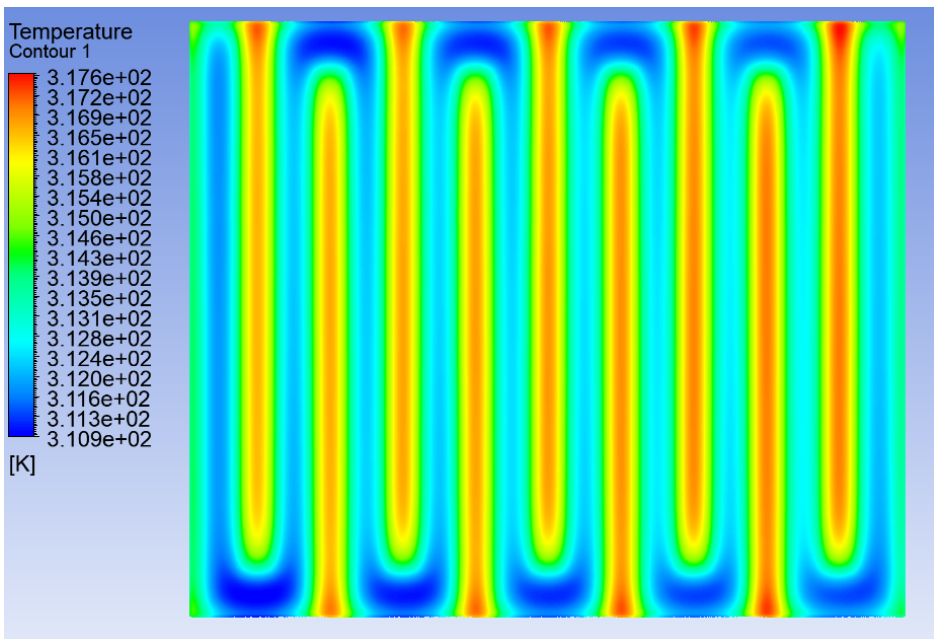


**Figure 19(b):** Temperature contour of PV panel with  $\text{Fe}_3\text{O}_4$  ( $\phi = 1.5$ ) flowrate at 5L/min,  
heat flux at  $700\text{W/m}^2$

In figure 19(a) the temperature contour of the fluid domain has been shown and in figure 19(b) the temperature contour of the photovoltaic panel has been shown. In the results of this simulation of  $\text{Fe}_3\text{O}_4$  ( $\phi = 1.5$ ) flowing at 5L/min and the heat flux set at  $700\text{W/m}^2$  PV panel temperatures ranged from a high of  $44.45^\circ\text{C}$  to a low of  $37.75^\circ\text{C}$ . The area weighted average temperature was  $40.95^\circ\text{C}$ . The calculated PMPP for this temperature is  $41.83\text{W}$  and the efficiency is  $13.15\%$

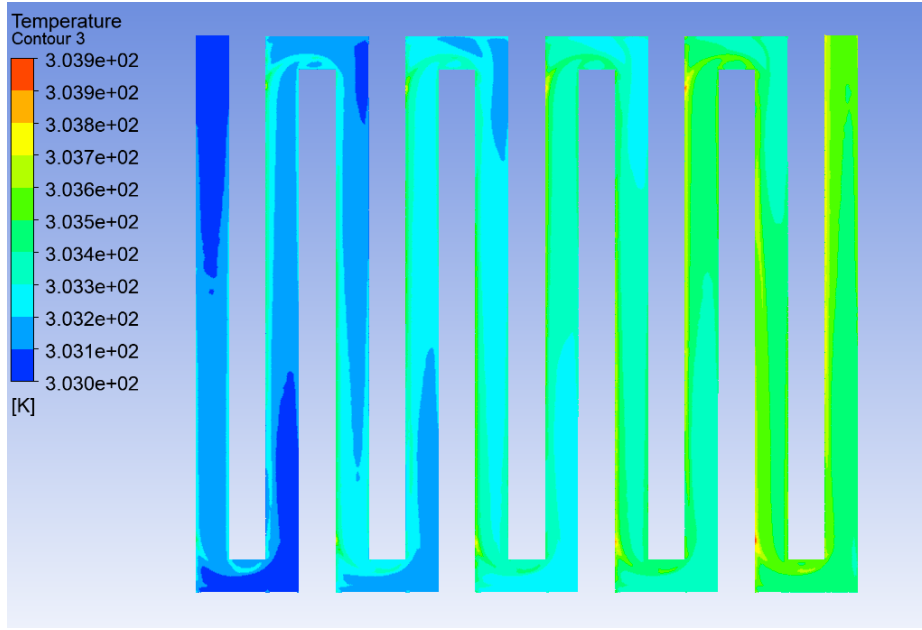


**Figure 20(a):** Temperature contour of  $\text{Fe}_3\text{O}_4$  ( $\phi = 1.5$ ) flowrate = 5L/min, heat flux = 500W/m<sup>2</sup>

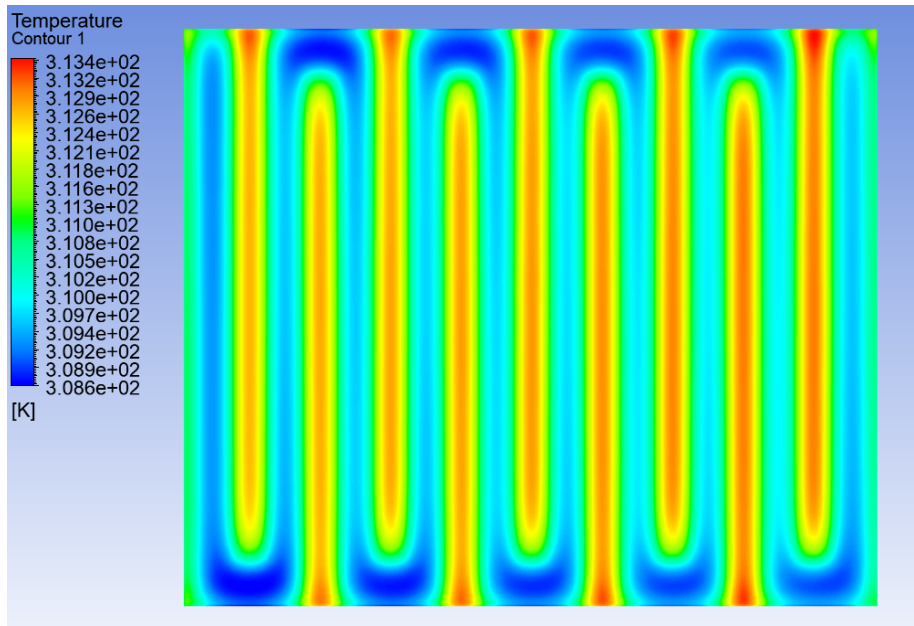


**Figure 20(b):** Temperature contour of PV panel with  $\text{Fe}_3\text{O}_4$  ( $\phi = 1.5$ ) flowrate at 5L/min, heat flux at 500W/m<sup>2</sup>

In figure 20(a) the temperature contour of the fluid domain has been shown and in figure 20(b) the temperature contour of the photovoltaic panel has been shown. In the results of this simulation of  $\text{Fe}_3\text{O}_4$  ( $\phi = 1.5$ ) flowing at 5L/min and the heat flux set at 500W/m<sup>2</sup>. The PV panel's highest recorded temperature was 40.25°C, while its lowest recorded temperature was 35.45°C. The area weighted average temperature was 37.79 °C. The calculated PMPP for this temperature is 42.47W and the efficiency is 13.36%

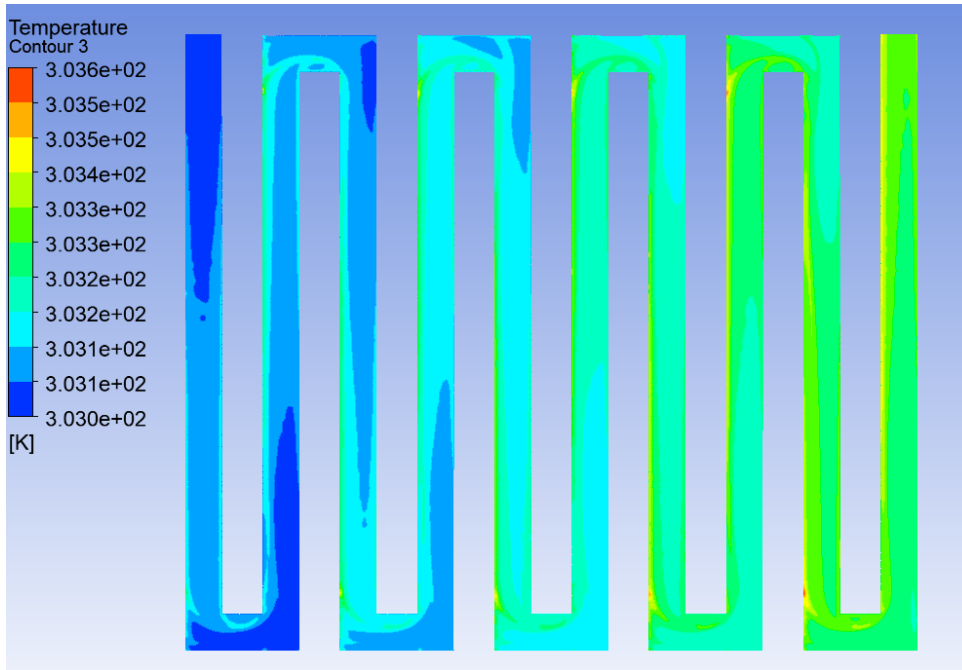


**Figure 21(a):** Temperature contour of  $\text{Fe}_3\text{O}_4$  ( $\varphi = 1.5$ ) flowrate = 5L/min, heat flux =  $300\text{W/m}^2$

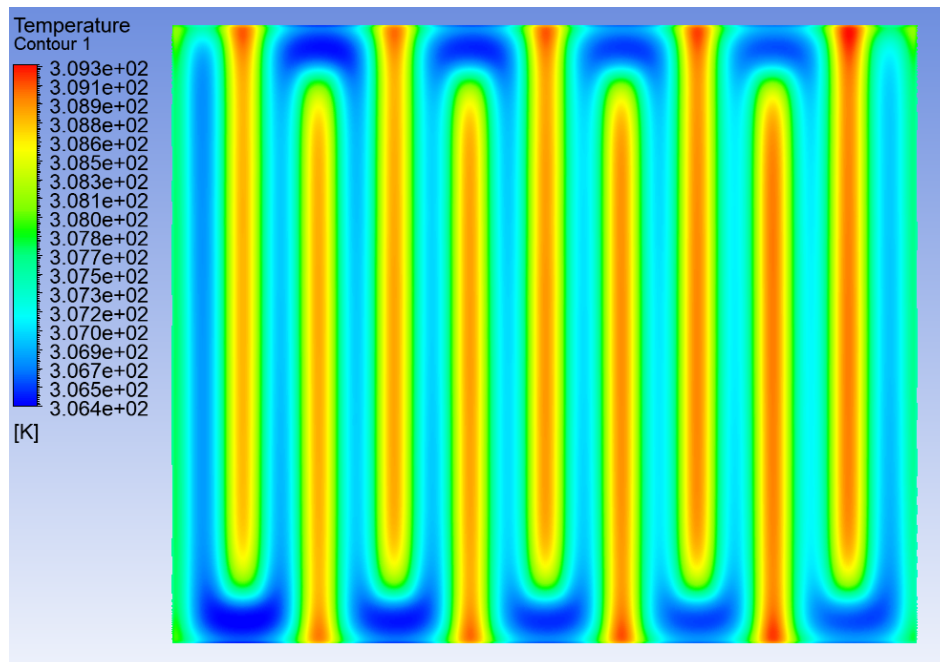


**Figure 21(b):** Temperature contour of PV panel with  $\text{Fe}_3\text{O}_4$  ( $\varphi = 1.5$ ) flowrate at 5L/min, heat flux at  $300\text{W/m}^2$

In figure 21(a) the temperature contour of the fluid domain has been shown and in figure 21(b) the temperature contour of the photovoltaic panel has been shown. In the results of this simulation of  $\text{Fe}_3\text{O}_4$  ( $\varphi = 1.5$ ) flowing at 5L/min and the heat flux set at  $300\text{W/m}^2$  The PV panel reached a high of  $36.15^\circ\text{C}$  and a low of  $33.25^\circ\text{C}$ . The area weighted average temperature was  $34.61^\circ\text{C}$ . The calculated PMPP for this temperature is  $43.12\text{W}$  and the efficiency is  $13.56\%$ .

**Table 3:** Compiled results of all the numerical simulation

Sl. no	Working Fluid	Area Weighted Average Temperature, K	PMPP(T), W	Efficiency
1	PV panel without cooling	483.87	7.378	2.32%
2	Water, flowrate = 1L/min	323.8924	39.8451	12.53%
3	Water, flowrate = 5L/min	320.4795	40.54	12.75%
4	Fe <sub>3</sub> O <sub>4</sub> ( $\phi = 0.2$ ), flowrate = 5L/min	320.264	40.6	12.77%
5	Fe <sub>3</sub> O <sub>4</sub> ( $\phi = 0.6$ ), flowrate = 5L/min	320.3195	40.57	12.75%
6	Fe <sub>3</sub> O <sub>4</sub> ( $\phi = 1$ ), flowrate = 5L/min	320.4643	40.54	12.75%
7	Fe <sub>3</sub> O <sub>4</sub> ( $\phi = 1.5$ ), flowrate = 5L/min	320.4495	40.54	12.75%
8	Fe <sub>3</sub> O <sub>4</sub> ( $\phi = 2$ ), flowrate = 5L/min	320.4195	40.55	12.75%
9	Fe <sub>3</sub> O <sub>4</sub> ( $\phi = 1.5$ ), flowrate = 4L/min	320.723	40.48	12.73%
10	Fe <sub>3</sub> O <sub>4</sub> ( $\phi = 1.5$ ), flowrate = 3L/min	321.1549	40.4	12.7%
11	Fe <sub>3</sub> O <sub>4</sub> ( $\phi = 1.5$ ), flowrate = 2L/min	321.8927	40.25	12.65%
12	Fe <sub>3</sub> O <sub>4</sub> ( $\phi = 1.5$ ), flowrate = 1L/min	323.8745	39.84	12.52%
13	Fe <sub>3</sub> O <sub>4</sub> ( $\phi = 1.5$ ), flowrate = 5L/min, Heat flux =900W/m <sup>2</sup>	317.29	41.185	12.95%
14	Fe <sub>3</sub> O <sub>4</sub> ( $\phi = 1.5$ ), flowrate = 5L/min, Heat flux =700W/m <sup>2</sup>	314.1	41.83	13.15%
15	Fe <sub>3</sub> O <sub>4</sub> ( $\phi = 1.5$ ), flowrate = 5L/min, Heat flux =500W/m <sup>2</sup>	310.94	42.47	13.36%
16	Fe <sub>3</sub> O <sub>4</sub> ( $\phi = 1.5$ ), flowrate = 5L/min, Heat flux =300W/m <sup>2</sup>	307.76	43.12	13.56%

Table 3 depicts the compiled result of all the simulations that were done in this paper. In total 16 simulations were done in this paper. The first case was photovoltaic panel without any cooling system. Then in the cases 2 and 3, water flowing at 1L/min and 5L/min were shown. In the cases 4-8 different volume fractions of Fe<sub>3</sub>O<sub>4</sub> were demonstrated. In the cases 9-12, different flowrates were demonstrated at the volume fraction of 1.5. All these cases from 1-12 were demonstrated at heat flux 1100W/m<sup>2</sup>. Now in the next 4 cases keeping the volume fraction at 1.5 and flowrate 5L/min, the simulations were done at varying heat fluxes.

## Chapter 6: Conclusion

The effectiveness of photovoltaic cells, photovoltaic thermal systems, thermal collector designs, and  $\text{Fe}_3\text{O}_4$  nanofluid are all examined in this work. ANSYS Fluent is used for computational fluid dynamics (CFD) based numerical analysis. The use of  $\text{Fe}_3\text{O}_4$  nanofluids improves the performance of solar panels coupled with thermal collectors. As a result of the nanofluids' characteristic value, with  $\text{Fe}_3\text{O}_4$ -based water-based PVT systems, the average PV temperature drops. This is due to the fact that nanofluids can speed up heat transfer, lowering temperatures to boost the performance of photovoltaic solar cells. The cell temperature of the PVT system is always less than the cell temperature of PV panels, regardless of the working fluid. The simulations performed for this paper reveal that the optimal configuration has a volume flowrate of 5 L/min, a concentration of 1.5 volume fraction of  $\text{Fe}_3\text{O}_4$ , and a heat flux of  $300 \text{ W/m}^2$ , whereas the inefficient configuration has no cooling medium present and achieves an efficiency of 2.32%.

Insights into the efficiency of several aspects, including solar cells, photovoltaic thermal systems, thermal collector designs, and the use of  $\text{Fe}_3\text{O}_4$  nanofluid, are provided by the findings of this study. These results open up numerous avenues for further study and development in the renewable energy and solar power industries. The implications of this finding for the future can be stated as follows:

The identified best configuration in this study can form the basis for future optimization research. To see if there are more efficient configurations, researchers can try varying the volume flow rate, concentration of  $\text{Fe}_3\text{O}_4$  nanofluid, and heat flux. It is possible to further improve the efficiency of solar panels combined with thermal collectors by conducting extensive optimization studies. The results of CFD simulations can be verified through additional experimental research, which is known as experimental validation. The effectiveness of  $\text{Fe}_3\text{O}_4$  nanofluids in enhancing the efficiency of photovoltaic solar cells may be verified by the construction of physical prototypes and the execution of real-world experiments. The proposed conclusions can be more credible and practical if they are experimentally validated. While this study's results using  $\text{Fe}_3\text{O}_4$  nanofluid are encouraging, future studies can investigate the use of different nanofluids and how they affect solar panel efficiency. Heat transfer and overall efficiency in photovoltaic thermal systems could benefit from further investigation into alternate nanofluids, such as those based on graphene or carbon nanotubes. Analyzing the long-term performance of photovoltaic thermal systems based on  $\text{Fe}_3\text{O}_4$  nanofluids would be very useful. Long-term performance monitoring will reveal important information about the

system's reliability, longevity, and overall efficiency. Maintenance and improvement plans can be better informed by the results of this investigation of possible degradation and aging impacts. Economic Viability and Technological Integration Future research can evaluate the commercial viability and scalability of incorporating photovoltaic thermal systems based on Fe<sub>3</sub>O<sub>4</sub> nanofluids. It will be vital for the general adoption of this technology to consider the cost-effectiveness, manufacturing feasibility, and ease of integration with existing solar energy infrastructure. It is crucial to assess the environmental impact of photovoltaic thermal systems based on Fe<sub>3</sub>O<sub>4</sub> nanofluid. The environmental and sustainability benefits of this technology compared to traditional photovoltaic systems can be better understood by analyzing elements like resource consumption, waste generation, and life cycle analysis. The findings of this study can help improve our understanding of how to best utilize solar power, leading to the creation of more effective and long-lasting energy solutions if we follow these lines of inquiry.

## References

- [1] Lee Y, Park C, Balaji N, Lee Y-J, Dao VA. High-efficiency silicon solar cells: a review. *Isr J Chem* 2015;55:1050–63, <https://dx.doi.org/10.1002/ijch.20140021>
- [2] Zainal Arifin, Singgih Dwi Prasetyo, Dominicus Danardono Dwi Prija Tjahjana, Rendy Adhi Rachmanto, Aditya Rio Prabowo, Noval Fattah Alfaiz, The application of TiO<sub>2</sub> nanofluids in photovoltaic thermal collector systems, *Energy Reports*, Volume 8, Supplement 9, 2022, Pages 1371-1380, ISSN 2352-4847, <https://doi.org/10.1016/j.egy.2022.08.070>
- [3] Gomaa MR, Ahmed M, Rezk H. Temperature distribution modeling of PV and cooling water PV/T collectors through thin and thick cooling cross-fined channel box. *Energy Rep* 2022;8:1144–53. <http://dx.doi.org/10.1016/j.egy.2021.11.061>
- [4] Barbu M, Siroux M, Darie G. Numerical model and parametric analysis of a liquid based hybrid photovoltaic thermal (PVT) collector. *Energy Rep* 2021;7:7977–88. <http://dx.doi.org/10.1016/j.egy.2021.07.058>.
- [5] Kazem HA. Evaluation and analysis of water-based photovoltaic/thermal (PV/T) system. *Case Stud Therm Eng* 2019;13:100401. <http://dx.doi.org/10.1016/j.csite.2019.100401>.
- [6] Al-Waeli AHA, Chaichan MT, Sopian K, Kazem HA, Mahood HB, Khadom AA. Modeling and experimental validation of a PVT system using nanofluid coolant and nano-PCM. *Sol Energy* 2019;177:178–91. <http://dx.doi.org/10.1016/j.solener.2018.11.016>.
- [7] R. Cazzaniga, M. Rosa-Clot, P. Rosa-Clot and G. M. Tina, "Floating tracking cooling concentrating (FTCC) systems," *2012 38th IEEE Photovoltaic Specialists Conference*, Austin, TX, USA, 2012, pp. 000514-000519, doi: 10.1109/PVSC.2012.6317668
- [8] H. Hashim, J.J. Bompfrey, G. Min, Model for geometry optimisation of thermoelectric devices in a hybrid PV/TE system, *Renewable Energy*, Volume 87, Part 1, 2016, Pages 458-463, ISSN 0960-1481, <https://doi.org/10.1016/j.renene.2015.10.029>.
- [9] Cătălin George Popovici, Sebastian Valeriu Hudișteanu, Theodor Dorin Mateescu, Nelu-Cristian Cherecheș, Efficiency Improvement of Photovoltaic Panels by Using Air Cooled Heat Sinks, *Energy Procedia*, Volume 85, 2016, Pages 425-432, ISSN 1876-6102, <https://doi.org/10.1016/j.egypro.2015.12.223>.
- [10] [4] Aarti Kane, Vishal Verma, Bhim Singh, Optimization of thermoelectric cooling technology for an active cooling of photovoltaic panel, *Renewable and Sustainable Energy*

Reviews, Volume 75, 2017, Pages 1295-1305, ISSN 1364-0321, <https://doi.org/10.1016/j.rser.2016.11.114>

[11] Shuang-Ying Wu, Qiao-Ling Zhang, Lan Xiao, Feng-Hua Guo, A heat pipe photovoltaic/thermal (PV/T) hybrid system and its performance evaluation, *Energy and Buildings*, Volume 43, Issue 12, 2011, Pages 3558-3567, ISSN 0378-7788, <https://doi.org/10.1016/j.enbuild.2011.09.017>.

[12] Jee Joe Michael, Iniyar S, Ranko Goic, Flat plate solar photovoltaic–thermal (PV/T) systems: A reference guide, *Renewable and Sustainable Energy Reviews*, Volume 51, 2015, Pages 62-88, ISSN 1364-0321, <https://doi.org/10.1016/j.rser.2015.06.022>.

[13] Mingke Hu, Renchun Zheng, Gang Pei, Yunyun Wang, Jing Li, Jie Ji, Experimental study of the effect of inclination angle on the thermal performance of heat pipe photovoltaic/thermal (PV/T) systems with wickless heat pipe and wire-meshed heat pipe, *Applied Thermal Engineering*, Volume 106, 2016, Pages 651-660, ISSN 1359-4311, <https://doi.org/10.1016/j.applthermaleng.2016.06.003>

[14] Sula Ntsaluba, Bing Zhu, Xiaohua Xia, Optimal flow control of a forced circulation solar water heating system with energy storage units and connecting pipes, *Renewable Energy*, Volume 89, 2016, Pages 108-124, ISSN 0960-1481, <https://doi.org/10.1016/j.renene.2015.11.047>

[15] J.K. Tonui, Y. Tripanagnostopoulos, Improved PV/T solar collectors with heat extraction by forced or natural air circulation, *Renewable Energy*, Volume 32, Issue 4, 2007, Pages 623-637, ISSN 0960-1481, <https://doi.org/10.1016/j.renene.2006.03.006>.

[16] Saeed Aghakhani, Masoud Afrand, Arash Karimipour, Rasool Kalbasi, Mohammad Mehdi Razzaghi, Numerical study of the cooling effect of a PVT on its thermal and electrical efficiency using a Cu tube of different diameters and lengths, *Sustainable Energy Technologies and Assessments*, Volume 52, Part A, 2022, 102044, ISSN 2213-1388, <https://doi.org/10.1016/j.seta.2022.102044>

[17] Govind S. Menon, S. Murali, Jacob Elias, D.S. Aniesrani Delfiya, P.V. Alfiya, Manoj P. Samuel, Experimental investigations on unglazed photovoltaic-thermal (PVT) system using water and nanofluid cooling medium, *Renewable Energy*, Volume 188, 2022, Pages 986-996, ISSN 0960-1481, <https://doi.org/10.1016/j.renene.2022.02.080>

[18] Saeed Aghakhani, Masoud Afrand, Experimental study of the effect of simultaneous



application of the air- and water-cooled flow on efficiency in a Photovoltaic thermal solar collector with porous plates, Applied Thermal Engineering, Volume 217, 2022, 119161, ISSN 1359-4311, <https://doi.org/10.1016/j.applthermaleng.2022.119161>

[19] Fahad Al-Amri, Taher S. Maatallah, Omar F. Al-Amri, Sajid Ali, Sadaqat Ali, Ijlal Shahrukh Ateeq, Richu Zachariah, Tarek S. Kayed, Innovative technique for achieving uniform temperatures across solar panels using heat pipes and liquid immersion cooling in the harsh climate in the Kingdom of Saudi Arabia, Alexandria Engineering Journal, Volume 61, Issue 2, 2022, Pages 1413-1424, ISSN 1110-0168, <https://doi.org/10.1016/j.aej.2021.06.046>

[20] Kadir Gelis, Kadir Ozbek, Ali Naci Celik, Omer Ozyurt, A novel cooler block design for photovoltaic thermal systems and performance evaluation using factorial design, Journal of Building Engineering, Volume 48, 2022, 103928, ISSN 2352-7102, <https://doi.org/10.1016/j.jobbe.2021.103928>

[21] Ahmad Zarei, Sohail Elahi, Hassan Pahangeh, Design and analysis of a novel solar compression-ejector cooling system with eco-friendly refrigerants using hybrid photovoltaic thermal (PVT) collector, Thermal Science and Engineering Progress, Volume 32, 2022, 101311, ISSN 2451-9049, <https://doi.org/10.1016/j.tsep.2022.101311>

[22] Hongkai Chen, Zeyu Li, Bin Sun, Performance evaluation and parametric analysis of an integrated diurnal and nocturnal cooling system driven by photovoltaic-thermal collectors with switchable film insulation, Energy Conversion and Management, Volume 254, 2022, 115197, ISSN 0196-8904, <https://doi.org/10.1016/j.enconman.2021.115197>

[23] Faruk Yesildal, Ahmet Numan Ozakin, Kenan Yakut, Optimization of operational parameters for a photovoltaic panel cooled by spray cooling, Engineering Science and Technology, an International Journal, Volume 25, 2022, 100983, ISSN 2215-0986, <https://doi.org/10.1016/j.jestch.2021.04.002>

[24] Rui Miao, Xiaou Hu, Yao Yu, Yan Zhang, Mark Wood, Gaylord Olson, Huojun Yang, Evaluation of cooling performance of a novel dual-purpose solar thermal collector through numerical simulations, Applied Thermal Engineering, Volume 204, 2022, 117966, ISSN 1359-4311, <https://doi.org/10.1016/j.applthermaleng.2021.117966>

[25] Talib K. Murtadha, Ali A. dil Hussein, Ahmed A.H. Alalwany, Saad S. Alrwashdeh, Ala'a M. Al-Falahat, Improving the cooling performance of photovoltaic panels by using two passes circulation of titanium dioxide nanofluid, Case Studies in Thermal Engineering,

Volume 36, 2022, 102191, ISSN 2214-157X, <https://doi.org/10.1016/j.csite.2022.102191>

[26] Mehrdad Ahmadinejad, Rouhollah Moosavi, Energy and exergy evaluation of a baffled-nanofluid-based photovoltaic thermal system (PVT), International Journal of Heat and Mass Transfer, Volume 203, 2023, 123775, ISSN 0017-9310, <https://doi.org/10.1016/j.ijheatmasstransfer.2022.123775>

[27] Fadli AF, Kristiawan B, Suyitno, Arifin Z. Analysis of TiO<sub>2</sub>/water-based photovoltaic thermal (PV/T) collector to improve solar cell performance. IOP Conf Ser Mater Sci Eng 2021;1096:012053. <http://dx.doi.org/10.1088/1757-899x/1096/1/012053>

[28] Jeonggyun Ham, Yunchan Shin, Honghyun Cho, Comparison of thermal performance between a surface and a volumetric absorption solar collector using water and Fe<sub>3</sub>O<sub>4</sub> nanofluid, Energy, Volume 239, Part C, 2022, 122282, ISSN 0360-5442, <https://doi.org/10.1016/j.energy.2021.122282>.

[29] L. Syam Sundar, Manoj K. Singh, Antonio C.M. Sousa, Investigation of thermal conductivity and viscosity of Fe<sub>3</sub>O<sub>4</sub> nanofluid for heat transfer applications, International Communications in Heat and Mass Transfer, Volume 44, 2013, Pages 7-14, ISSN 0735-1933, <https://doi.org/10.1016/j.icheatmasstransfer.2013.02.014>.

[30] Bazdidi-Tehrani F, Khabazipur A, Vasefi SI. Flow and heat transfer analysis of TiO<sub>2</sub>/water nanofluid in a ribbed flat-plate solar collector. Renew Energy 2018;122:406–18. <http://dx.doi.org/10.1016/j.renene.2018.01.056>.

[31] Elaheh Esmaeili, Reza Ghazanfar Chaydareh, Seyyed Amin Rounaghi, The influence of the alternating magnetic field on the convective heat transfer properties of Fe<sub>3</sub>O<sub>4</sub>-containing nanofluids through the Neel and Brownian mechanisms, Applied Thermal Engineering, Volume 110, 2017, Pages 1212-1219, ISSN 1359-4311, <https://doi.org/10.1016/j.applthermaleng.2016.09.014>.

[32] Prasetyo SD, Prabowo AR, Arifin Z. The effect of collector design in increasing PVT performance: Current state and milestone. Mater Today Proc 2022. <http://dx.doi.org/10.1016/j.matpr.2021.12.356>

[33] Arifin Z, Tjahjana DDDP, Hadi S, Rachmanto RA, Setyohandoko G, Sutanto B. Numerical and experimental investigation of air cooling for photovoltaic panels using aluminum heat sinks. Int J Photoenergy 2020;2020:1–9. <http://dx.doi.org/10.1155/2020/1574274>

- [34] Baranwal NK, Singhal MK. Modeling and simulation of a spiral type hybrid photovoltaic thermal (PV/T) water collector using ANSYS. In: Adv. clean energy technol. Singapore: Springer; 2021, p. 127–39. [http://dx.doi.org/10.1007/978-981-16-0235-1\\_10](http://dx.doi.org/10.1007/978-981-16-0235-1_10)
- [35] Kristiawan B, Kamal S. Thermo-hydraulic characteristics of anatase titania nanofluids flowing through a circular conduit. *J Nanoscience Nanotechnology* 2016;16:6078–85. <http://dx.doi.org/10.1166/jnn.2016.10902>
- [36] Mohammad H. Moradi, Ali Reza Reisi, A hybrid maximum power point tracking method for photovoltaic systems, *Solar Energy*, Volume 85, Issue 11, 2011, Pages 2965-2976, ISSN 0038-092X, <https://doi.org/10.1016/j.solener.2011.08.036>.
- [37] Nituca C, Chiriac G, Cuciureanu D, Zhang G, Han D, Plesca A. Numerical analysis of a real photovoltaic module with various parameters. *Model Simul Eng* 2018;2018. <http://dx.doi.org/10.1155/2018/7329014>.
- [38] Kasaeian A, Khanjari Y, Golzari S, Mahian O, Wongwises S. Effects of forced convection on the performance of a photovoltaic thermal system: An experimental study. *Exp Therm Fluid Sci* 2017;85:13–21. <http://dx.doi.org/10.1016/j.expthermflusci.2017.02.012>
- [39] Mohammad H. Moradi, Ali Reza Reisi, A hybrid maximum power point tracking method for photovoltaic systems, *Solar Energy*, Volume 85, Issue 11, 2011, Pages 2965-2976, ISSN 0038-092X, <https://doi.org/10.1016/j.solener.2011.08.036>
- [40] Arifin Z, Tjahjana DDDP, Hadi S, Rachmanto RA, Setyohandoko G, Sutanto B. Numerical and experimental investigation of air cooling for photovoltaic panels using aluminum heat sinks. *Int J Photoenergy* 2020;2020:1–9. <http://dx.doi.org/10.1155/2020/1574274>



## PAPER NAME

180011206\_Naimul Islam.docx

## WORD COUNT

8923 Words

## CHARACTER COUNT

50109 Characters

## PAGE COUNT

45 Pages

## FILE SIZE

12.8MB

## SUBMISSION DATE

May 26, 2023 1:47 PM GMT+6

## REPORT DATE

May 26, 2023 1:48 PM GMT+6


**● 15% Overall Similarity**

The combined total of all matches, including overlapping sources, for each database.

- 9% Internet database
- Crossref database
- 11% Submitted Works database
- 9% Publications database
- Crossref Posted Content database

**● Excluded from Similarity Report**

- Bibliographic material
- Cited material



Approved  
Dr. Md. Rezwanul Karim  
Associate Professor  
Department of Mechanical and Production Engineering  
Islamic University of Technology (IUT), OIC  
Board Bazar, Gazipur-1714 Bangladesh